USDOT Region V Regional University Transportation Center Final Report

NEXTRANS Project No. 047IY02

Traffic Signal Coordination and Queue Management in Oversaturated Intersection

By

Ali Hajbabaie

PhD Candidate

University of Illinois at Urbana Champaign

ahajbab2@illinois.edu

And

Juan C. Medina

PhD Candidate

University of Illinois at Urbana Champaign

jcmedina@Illinois.edu

And

Rahim F. Benekohal (PI)

Professor

University of Illinois at Urbana Champaign

rbenekoh@illinois.edu

Report Submission Date: March 18, 2011

DISCLAIMER

Funding for this research was provided by the NEXTRANS Center, Purdue University under Grant No. DTRT07-G-005 of the U.S. Department of Transportation, Research and Innovative Technology Administration (RITA), University Transportation Centers Program. The contents of this report reflect the views of the authors, who are responsible for the facts and the accuracy of the information presented herein. This document is disseminated under the sponsorship of the Department of Transportation, University Transportation Centers Program, in the interest of information exchange. The U.S. Government assumes no liability for the contents or use thereof.

USDOT Region V Regional University Transportation Center Final Report

TECHNICAL SUMMARY

NEXTRANS Project 047IY02 Final Report, March 2011

Traffic Signal Coordination and Queue Management in Oversaturated Intersections

Introduction

Traffic signal timing optimization when done properly, could significantly improve network performance by reducing delay, increasing network throughput, reducing number of stops, or increasing average speed in the network. The optimization can become complex due to large solution space caused by many combinations of different parameters that affect traffic operation. In this study three different methods are used to find near-optimal signal timing parameters in transportation networks. The methods are: Genetic Algorithms (GA), Evolution Strategies (ES), and Approximate Dynamic Programming (ADP). Each method is introduced, the signal timings associated with them are explained and some important measures of performance of the networks are determined and compared. One small network with 9 intersections and one medium network with 20 intersections were used for evaluating the optimizations methods. Three general cases (Cases 1, 2, 3) are discussed in this report. For the small symmetric network, three levels of traffic loading are used (no overload, 10% overload and 20% overload). For the medium network (modified Springfield IL downtown network), two levels of entry volumes are used (750 and 1000 vehicle per hour per lane).

Findings

On the small network of nine oversaturated intersections GA and ES methods were use to find optimal solutions for three network loading conditions (no overloading, 10%, and 20% overloading). Also two variations of ADP (no eligibility traces and eligibility traces) and three

modified ADP algorithms were tested for the small network. The results indicated that GA and ES with no overloading and two variations of ADP and their modifications found signal timings that resulted in similar network performances. From these four cases, the average delay was between 215 to 226 seconds per vehicle. The ADP Modification 3 resulted in the lowest average delay and ADP with eligibility traces resulted in the highest. System throughput was also similar and ranged from 2095 vehicle (ES with 20% overloading) to 2320 vehicles (ADP with no eligibility traces). When the network was overloaded by 10% or 20%, average delay per vehicles significantly increased while system throughput was still at the same level or slightly lower.

In comparison, the signal timings for the small network found by GA and ES were similar and resulted in cycle lengths that fluctuated between 78 and 98 seconds (with identical averages of 85 seconds). However, the ADP method (with and without eligibility traces), found cycle lengths of 85 to 107 seconds when left turns phases were displayed, and cycle lengths of 50 to 63 seconds when left turn phases did not exist.

For the modified Springfield network, when the volumes at the entry links were 750 vehicles per hour per lane GA and ADP found average delays of 70.3 sec and 75.8 sec, respectively, and were shorter that average delay of 78.7 s for ES and 85.6 s for the modified ADP. Network throughputs for GA (4987 vehicles), ES (5005 vehicles), and ADP (4981 vehicles) were similar and slightly higher than that for modified ADP (4746 vehicles). Higher throughput and lower delay for GA and ES was expected since they were optimizing the offsets in addition to signal timing parameters, and as a result several intersections end up having signal coordination. ADP on the other hand was responding to the current network condition assuming the intersections were not interconnected. The signal coordination resulted in less number of stops in the network and increased average speed. Thus, average number of stops for GA (2.0 stops) and ES (2.4 stops) were fewer than that for ADP (3.0) and its modification (3.3). In addition, GA (14.0 mph), ES (12.9 mph), and ADP (13.1 mph) resulted in a higher average speed in the network than modified ADP (12.1 mph).

When the entry volumes were set to 1000 in the modified Springfield network, GA and ES could coordinate some of the signals of the network. As a result, average delay inside the network for

GA (144 s) and ES (137 s) was shorter than that for ADP (159 s) and modified ADP (171 s). However, GA and ES metered vehicles at the entry links more than ADP and its modification and did not let too many vehicles enter the network. This resulted in a larger total average delay (inside and outside) of the network for GA (227 s) and ES (222 s) compared to ADP (187 s) and modified ADP (203 s). Since GA and ES let fewer number of vehicles enter the network, the throughput for ADP (4718 vehicles) was more than that for GA (4302 vehicles) and ES (4388 vehicles). On the other hand, since the links and intersections inside the network were not as congested, the average number of stops was lower for GA (4.2 stops) and ES (4.1 stops) compared to ADP (5.1 stops) and modified ADP (5.1 stops). Similarly, and average speed was higher for GA (8.2 mph) and ES (8.6 mph) than ADP (7.5 mph) and modified ADP (7.0 mph) modified ADP.

Queue management is more important than delay minimization in oversaturated network. For queue management purposes, we simultaneously considered the efficiency of green utilization and queue occupancy in assessing the effectiveness of the signal timing optimization methods used in this study. The queue management analysis showed that to get the best network performance in the oversaturated condition, the green utilization efficiency for protected movements (through or left-turns) should be close to saturation headway.

In addition, it was found that letting too many vehicles enter into an oversaturated network is not be the best strategy for all traffic conditions. Vehicles could enter the network up to a certain traffic demand, but beyond this point the network will not be able to process them and blockage or gridlocks may happen. This may in turn result in a decrease in the number of trips, and an increase in average travel delay both inside the network and at the borders. Whenever traffic demand is beyond this optimal level, the traffic demand should be metered to prevent a network overload and decrease in the network throughput.

Recommendations

Future work to improve the methods described in the report, particularly for real-world applications, is needed. Several topics can be further studied for advancing the state-of-the-

practice in traffic signal control, including: 1) reduction in the required running time for GA and ES, 2) improvements in the algorithm for ADP regarding the state representation and the learning functions, 3) the long term performance of the algorithms, and 4) extended capabilities such as communication between intersection and augmented set of constraints to account for known issues in real-world scenarios.

Contacts

For more information:

Professor Rahim F. Benekohal
University of Illinois at Urbana Champaign
205 N Mathews Ave
Urbana, IL, 61801
Phone number: 217-244-6288
Fax number: 217-333-1924
Email Address: rbenekoh@illinois.edu

NEXTRANS Center
Purdue University - Discovery Park
2700 Kent B-100
West Lafayette, IN 47906

nextrans@purdue.edu
(765) 496-9729
(765) 807-3123 Fax

www.purdue.edu/dp/nextrans

NEXTRANS Project No. 047IY02

Traffic Signal Coordination and Queue Management in Oversaturated Intersection

By

Ali Hajbabaie
PhD Candidate
University of Illinois at Urbana Champaign
ahajbab2@illinois.edu

And

Juan C. Medina
PhD Candidate
University of Illinois at Urbana Champaign
jcmedina@Illinois.edu

And

Rahim F. Benekohal (PI)
Professor
University of Illinois at Urbana Champaign
rbenekoh@illinois.edu

Report Submission Date: March 18, 2011

Contents

CHAPTER 1. INTRODUCTION

Transportation demand has continued to increase over the past years. Traffic congestion in major US metropolitan areas costs $87 billion dollars annually (Schrank & Lomax, 2009). This cost plus other negative effects of traffic congestion, calls for practical methods to better manage transportation networks. An effective method to reduce congestion is transportation supply management, which can be implemented in the form of optimal or near-optimal signal timing parameters in a network (i.e. cycle length, phase plane, green splits, and offsets).

It is well known that solving the problem of finding optimal signal timings for a network, particularly in oversaturated conditions, is very challenging. This is the case because the signal timing at one intersection influences the state of other intersections, and also because no closed-form expressions are available for network delay and throughput based on signal timing parameters.

Consider for example a network of 20 intersections with protected left turn phases, two-way streets, fixed signal timing (i.e. cycle length, green splits, and offsets do not change in the study period), and a study period of 15 minutes. This simple case will result in a decision space as large as 1.86×10^{153}, when combining all possible signal timings. More specifically, at each intersection with a four-phase signal plan, there are 8 different values for left turns for each direction (assuming a minimum of 7 seconds and a maximum of 15 seconds), 60 different values for through movement at each direction (assuming a minimum of 20 seconds and a maximum of 80 seconds), and 200 different values for offsets (assuming

a minimum of 0 seconds and maximum of 200 seconds). The combination of these solutions yields $(8\times60\times8\times60\times200)^{20}$, or 1.86×10^{153}.

Therefore, traditional optimization methods either do not find the optimal solution (since the objective function does not have a closed-form formulation), or they need an extraordinary amount of time to find an optimal solution.

On the other hand, meta-heuristic approaches such as Genetic Algorithms (GA), and Evolution Strategies (ES), and intelligent learning approaches such as Approximate Dynamic Programming (ADP) could be coupled with a microscopic traffic simulation tool to effectively determine optimal or near-optimal signal timing parameters in a transportation network.

Thus, in this study, these approaches (GA, ES, and ADP) are used to solve the abovementioned problem; they are individually described, analyzed, and also compared to each other.

This report is divided into 7 chapters. Chapter 2 contains a critical review of relevant literature. In Chapter 3 the methodology of the study is presented. Chapter 4 describes the case study networks used in this study. Chapter 5 explains signal timing parameters found by each search technique. In Chapter 6 the effects of different strategies on the network performance are described and Chapter 6 presents the concluding remarks and future work.

CHAPTER 2. BACKGROUND

Traffic signal timing, when done properly, improves intersection traffic operation and safety. The majority of traffic signal optimization methods use the concept of delay minimization either alone or in combination with other factors. Delay minimization works well in undersaturated conditions where queue spillbacks do not block the adjacent lanes or nearby intersections. A few popular software programs (Synchro, PASSER, TRANSYT7F, MAXBAND, etc) provide signal coordination plans using the delay minimization concept. The demand-responsive signal coordination methods such as Split, Cycle, Offset, Optimization Technique (SCOOT) and Sydney Coordinated Adaptive Traffic System (SCATS) are also based on delay minimization concept. Furthermore, the adaptive methods such as Optimization Policy for Adaptive Control (OPAC) and Real-time Hierarchical Optimized Distributed Effective System (RHODES) are also based on delay minimization. All these techniques work in undersaturated conditions where demand is less than the capacity and usually the queue dissipates before the green signal ends.

However, in oversaturated conditions, the queues would not completely dissipate after the green signal. In this case if they are not managed properly, they may grow and eventually block an upstream signal, resulting in a gridlock. To prevent this, queues in an oversaturated network should be carefully monitored, and the optimization technique should take queues into account either in the objective function, or in the constraints.

In the rest of this section the previous studies on signal timing optimization in oversaturated condition will be reviewed.

Early studies on signal control in oversaturated conditions were done by Gazis (1964), and Gazis and Potts (1965). Gazis proposed a method to control two closely-located oversaturated intersections and minimized delay (Gazis D. C., 1964) (Gazis & Potts, 1965).

Michalopoulos and Stephanopoulos (1977) used control theory to propose a strategy to minimize delay on a single, and on two oversaturated intersections with one-way streets. Their study considered queue constraints, travel time between the two intersections, and turning movements. (Michalopoulos & Stephanopoulos, 1977).

Lo and chow (2004) applied their Dynamic Intersection Signal Control Optimization (DISCO) method to a one-way arterial. DISCO uses the cell transmission model proposed by Daganzo (1992) and simple genetic algorithms to find near-optimal signal timing. They found that the most flexible strategy plan, variable-green-no-cycle, did not necessarily result in the best answer under the limitations of solution heuristics, especially when no good initial solutions were provided. However, with good initial signal timing, this plan outperformed other plans. (Lo & Chow, 2004) (Daganzo, 1992).

Yuan et al. (2006) determined optimal signal timing in a network of three intersections for an oversaturation period of ten minutes. They used cell transmission model, and Genetic Algorithms (GA) to find the optimal signal timing. Their algorithm used a fixed-cycle strategy and determined signal timing parameters. They found that the best signal timing with fixed-cycle strategy has a cycle length that is less than the maximum cycle length. This findings contrasted with other previous studies (Yuan, Yang, & Shen, 2006).

Abu-lebdeh and Benekohal (1999) developed a dynamic traffic signal control procedure for oversaturated arterials. Their method produced real-time signal timings that dynamically managed queue formation and dissipation. For a one-way arterial, their method provided dynamic time-dependent traffic control. Offsets and green times were dynamically changed as a function of demand and queue lengths. They found similar results for a two-way arterial however, as expected, for the secondary direction their algorithm could not provide all the capabilities associated with the primary direction (Abu-Lebdeh & Benekohal, 1997) (Abu-Lebdeh & Benekohal, 2000).

Park et al. (2000) used genetic algorithms to optimize signal timing of oversaturated intersections and tested their method on an arterial of four intersections. They used three objective functions that were: delay minimization, modified delay minimization with penalty function, and throughput maximization. They found that the GA-based algorithm with delay minimization produced a superior signal timing compared to other GA strategies and TRANSYT-7F (Park, Messer, & Urbanik II, 2000).

Lieberman et al. (2010) proposed a signal control optimization policy that was designed only for oversaturated condition. Their method maximized throughput while managing queues in the system. They tested their model on a one-way oversaturated arterial of two intersections and stated that their model provided an overall higher utilization of intersection capacity, consistently better service for cross streets and 22% lower delay per vehicle compared to TRANSYT-7F (Lieberman, Chang, Bertoli, & Wuping, 2010).

Zhang et al. (2010) proposed and offline method to determine signal timing for a pre-timed two-way arterial of five oversaturated intersections. Their method determined fixed signal timing for their study period. They used cell transmission models and GA and determined cycle length, green splits, phase sequence, and offsets to minimize the expected delay incurred by "high-consequence" demand scenarios. They found their method working better against high-consequence demand scenarios without losing optimality in the average sense (Zhang, Yin, & Lou, 2010).

Li and Chang (2010) proposed a model for signal optimization in an arterial with enhanced cell transmission formulation that worked in both undersaturated and oversaturated condition. They introduced a new diverging cell for formulating interactions of queue spillback between through traffic and left turn. They stated that their model yielded effective signal plans for undersaturated and oversaturated intersections (Li & Chang, 2010) .

Xin et al. (2010) developed a new adaptive signal control decision support system. Their system could operate in two modes one with operator in the loop and one without the operator or autonomous. Based on simulation results they found that their method decreased the travel time by 8%. Based on the preliminary results, queue distribution was more balanced when their model was used (Xin, Chang, Bertoli, & Talas, 2010).

Longley (1968) proposed a method that was only applicable to oversaturated and saturated conditions. His method managed the queues so that a minimum number of secondary intersections were blocked. His algorithm worked by changing the green split between a maximum and a minimum so that the queue unbalanced was reduced to zero. Simulation studies found Longley's algorithm effective in saturated or oversaturated condition however, if any of the intersections became undersaturated, the algorithm would not be applicable anymore (Longley, 1968).

Singh and Tamura (1974) used optimal control theory to control traffic in oversaturated condition. Their method did not take the interference of downstream queues with upstream discharge into account. They assumed that the offsets were known. This assumption could be a limitation of their study since in oversaturated condition when queues were formed the interference with the upstream signal was not avoidable (Singh & Tamura, 1974).

D'ans and Gazis (1976) extended the work of Gazis (1964) for any number of signals and not only for one cycle. They used fixed time signals and minimized the lost time by vehicles in queues over the entire study period. They found that solving oversaturation problems required optimum allocation of routes to drivers, and optimum signal switching at each intersection, simultaneously (D'Ans & Gazis, 1976).

Girianna and Benekohal (2002) proposed dynamic signal coordination models for oversaturated transportation networks. They formulated the model as a dynamic optimization problem with the objective of maximizing the total number of vehicles released by the network and penalizing it by queue accumulation along the arterials and used genetic algorithms to find the near optimal signal timing. They found that their model successfully managed queues along the coordinated arterials and also created opportunity for traffic progression in specified directions (Girianna & Benekohal, 2002).

Chang and Sun (2003) proposed their method to dynamically control an oversaturated traffic signal network by using a bang-bang like model for oversaturated intersections, and TRANSYT-7F for undersaturated intersections. They tested their model in a network of 12 oversaturated intersections that were surrounded by 13 undersaturated intersections and they

allowed turning movements and compared it to TRANSYT-7F. They found that their method provided better results than TRANSYT-7F (Chang & Sun, 2004).

Sun and Benekohal (2006) developed a bi-level programming formulation and a heuristic solution for traffic control in an oversaturated network with dynamic demand and stochastic route choice. They used genetic algorithms and a cell transmission based incremental logit assignment to solve the problem and tested their method on two transportation networks. Using dynamic signal timing, reduced the average link travel time by 5-8% and up to 14% compared to a static signal timing (Sun, Benekohal, & Waller, 2006).

Putha et al. (2010) used ant colony optimization to solve signal coordination problem for an oversaturated network. Their formulation and case study network was very similar to Girianna and Benekohal's (2002) formulations and case study. They compared the performance of these two methods by comparing the average value of fitness function over 30 runs. They found that for most of the cases ant colony provided higher fitness compared to simple genetic algorithm except for the case with 400 population size/ants and 50 generations/trials (Putha, Quadrifoglio, & Zechman, 2010).

Regarding the use of dynamic programming (DP), only a few attempts at solving the problem of optimal signal timings in a traffic network are found in the literature. This is not surprising because even though DP is a tool to solve complex problems by breaking them down into simpler ones, it suffers from what is known as the curses of dimensionality. This is the result of generating a sequence of optimal decisions by moving backward in time to find exact global solutions. However, solving Belman's optimality equation in a recursive way can be computationally intractable, since it required the computation of nested loops over the whole state space, the action space, and the expectation of a random variable. In addition, DP requires knowing the precise transition function and the dynamics of the system over time, which can also be a major restriction for some applications.

Thus, with these considerations, finding limited literature for medium or large-sized problems exclusively using DP is not surprising. The work of Robertson and Bretherton (1974) and Gartner (1983) is cited as an example, where they found a 56% decrease in delays using DP compared to the best fixed-time plans.

On the other hand, Approximate Dynamic Programming (ADP) has increased potential for large-scale problems. ADP uses an approximate value function that is updated as the system moves forward in time, giving the advantage of an algorithm that increasingly improves an estimate of the value of a state. ADP can also effectively deal with stochastic conditions by using post-decision variables, as it will be explained in more detail in the subsequent sections.

Despite the fact that ADP has been used extensively as an optimization technique for a variety of fields, the literature shows only a few studies in signal timing optimization using this approach. Nonetheless, the wide application of ADP in other areas has shown that it can be a practical tool for real-world optimization problems, such as signal control in urban traffic networks.

A recent study on traffic control in a single intersection by Cai et al. (2009) used ADP with two different learning techniques: temporal-difference reinforcement learning, and perturbation learning. They reduced the delay from 13.95 vehicle-second per second (obtained with TRANSYT) to 8.64 vehicle-second per second. Also, a study by Teodorvic (2006) combined dynamic programming with neural networks for a real-time traffic adaptive signal control, claiming that the outcome of their algorithm was nearly equal to the best solution.

CHAPTER 3. METHODOLOGY

In this section, the principles used by Genetic Algorithms (GA), Evolution Strategies (ES), and Approximate Dynamic Programming (ADP) are described, as well as the details on how they are implemented to find optimal signal timing parameters in a traffic network.

3.1 Genetic Algorithms (GA)

GAs are search techniques to find exact or approximate solutions to an optimization or a search problem. GAs are global search meta-heuristics that are less likely to be trapped in a local optimum. GAs are a specific class of evolutionary algorithms and use techniques inspired by evolutionary biology such as inheritance, selection, crossover, and mutation.

GAs are implemented in a computer simulation environment where a population of candidate solutions are created and evolved towards better solutions over different generations. Unlike other well-known optimization techniques that start the search with one feasible solution, GAs start the search with several points in the feasible area. The initial population can be created randomly or by using some heuristics. Each population member is called an individual, or a chromosome, and has a fitness value that represents the value of the objective function for that individual. For example, if the objective function is to maximize $f(x) = x^2$, the fitness of the individual $x = 3$ will be $3^2 = 9$. Based on the fitness values, GAs stochastically select some individuals from the population, in such a way that higher fitness results in higher probability of being selected. The selected individuals form a mating pool where they are crossed over and mutated, and then they form some new individuals for the population in the next generation. GAs continue to select new individuals as parents until

enough individuals for the next generation are created. As soon as a new individual is created the fitness value of that individual is evaluated. The whole process of selection, crossover, and mutation is continued until the termination criteria are met. Usually a maximum number of generations, or a threshold for the relative difference between the maximum fitness value and average fitness value of a population are chosen as the termination criterion.

Simple GA uses binary coding to represent decision variables. This means that a decision variable in the form of $\vec{x} = (x_1, x_2, x_3, \dots, x_{m-1}, x_m)$ is represented as the following chromosome:

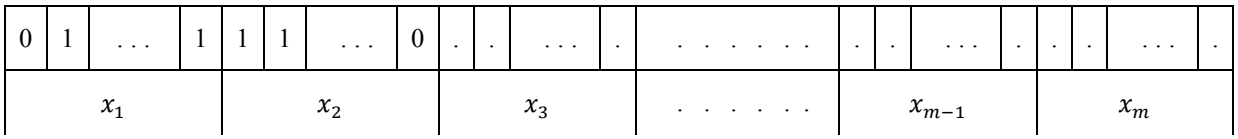

Figure 3.1. Binary representation of decision variables in GAs.

Simple GA has three operators: Selection, Crossover, and Mutation. In simple GA the initial population is created randomly or by using some heuristics. Then selection operator chooses two parents. These parents are crossed over, leading to two new individuals, which are mutated to form two individuals for the next generation. The three operators of simple GA are explained next:

3.1.1 **Selection**

Selection is one of the simple GA (and other variations of GAs) operators that leads the search to more desired parts of the feasible area. It simply selects the individuals with higher values; however, the process of selection is stochastic rather than deterministic. This process is not purely random but, is biased towards selection of individuals with higher fitness values. There are three main variations of selection:

3.1.1.1 Proportionate Selection

3.1.1.2 Truncation Selection

3.1.1.3 Tournament Selection

In this study a tournament selection with replacement with a pressure of 6.7% is used.

3.1.2 **Crossover**

Crossover (also called recombination) is one of GA's operators that results in reproducing new generation. In GAs, crossing over two parents leads to two new individuals that could potentially be fitter than their parents. To generate two new individuals by crossover, two parents are randomly selected from the mating pool and then crossed over. Several variations of cross over exist four of which are listed bellow:

3.1.2.1 Single-Point Crossover

3.1.2.2 Two-Point Crossover

3.1.2.3 Multi-Point Crossover

3.1.2.4 Uniform Crossover

In this study we have used a uniform cross over that selects each chromosome of the offspring probabilistically from one of the parents.

3.1.3 **Mutation**

Mutation is used in GAs to introduce more diversity to the search. In addition, if the parents are similar, crossing them over does not produce a new individual. In this case mutation is needed to generate a new offspring. In bitwise mutation, each bit of the chromosome is flipped according to the probability of the mutation. This means that, each bit of a chromosome is flipped with probability of Pm that is probability of mutation. Different methods of mutation exist. But in this research the regular mutation is used.

3.2 Evolution Strategy (ES)

ES, genetic algorithms, and evolutionary programming are the main three paradigms of Evolutionary Computation. In general, these three methods are based on iterative birth

and death, variation, and selection. The first ES had only two rules: 1) slightly change all variables at a time at random, 2) if this set of variables leads to better results keep them otherwise, keep the original ones. As it is apparent from the rules, this ES worked with only two individuals per iteration: one old individual or parent, and one new individual or offspring. This ES was later called 1+1-ES meaning that out of a single parent, one offspring is generated and among these two individuals, the best one is chosen. The 1+1-ES with binomially distributed mutations on a two dimensional parabolic ridge was studied by Schwefel (Schwefel, 1965). The study showed that 1+1-ES could get stuck in a local optimum. In this case, larger mutations were needed to escape from this local optimum. To solve this problem, instead of using discrete variables, using continuous variable with Gaussian distributions was suggested. Rechenberg presented approximate analyses of the 1+1-ES with Gaussian mutation on two different functions (hyper sphere, and rectangular corridor models). He found that the convergence was inversely proportional to the number of variables; linear convergence might be obtained if the mutation step size was set to the proper order of magnitude; and the optimal mutation strength was in the order of one fifth for both models. In addition, instead of using a single parent, he used μ, crossed them over, and generated one offspring. He concluded that this method could speed up the evolution if the speed was measured per generation; and the population might learn by itself how to adjust the mutation step size. This method of ES was called μ+1-ES since among μ+1 individuals the best μ individuals were selected or in other words, the worst individual is extinct. Later, μ+1-ES was expanded to $\mu+\lambda$-ES. In this method instead of creating a single offspring out of the μ parents, λ descendants are created. Then among these $\mu+\lambda$ individuals the μ fittest individuals are chosen to form the next population. Another variation of ES with $\mu>1$ parents and $\lambda>1$ descendants exists. In this method, after creating the new λ descendants, all parents are discarded. Out of the λ descendants, the fittest μ are chosen to form the next population. Thus, λ has to be strictly larger than λ. This method is called μ,λ-ES. In general, $\mu+\lambda$-ES and μ,λ-ES generate better results than $1+1$-ES and $\mu+1$-ES do. Although intuitively it is believed that $\mu+\lambda$-ES generates better results that μ,λ-ES does, for small μ and λ-*to*-μ ratio, μ,λ-ES generates better results. When μ and λ-*to*-μ ratio increase, both algorithms perform similarly.

All variations of ES with $\mu>1$ parents and $\lambda>1$ descendants have three different operators that are recombination, mutation, and selection. ES could be self adaptive. This means that as the populations evolve, the strategy parameters evolve as well. This is done by coupling of endogenous strategy parameters with the objective parameters. In other words, the decision vector contains object parameters as well as endogenous strategy parameters. This is shown in the equation below.

$$\overrightarrow{a_k} = (y_{1k}, y_{2k}, \dots, y_{Dk}, s_{1k}, s_{2k}, \dots, s_{Dk})$$

Where : y_{ij}: the i^{th} component of decision variable j, and

S_{ij}: the i^{th} component of endogenous strategy parameter j.

ES operators are briefly explained below:

3.2.1 **Recombination**

In recombination, $\rho \geq 1$ individuals among parents are selected and then recombined. When $\rho = 1$, the new offspring is simply equal to its parent meaning that no recombination is done. There are two main methods of recombination: discrete, and intermediate. In this study both methods have been used.

3.2.2 **Mutation**

Mutation is the main source of genetic variation in ES. The design of mutation operator is problem dependent. It is suggested that each mutation operator has to have reachability, unbiasedness, and scalability (Beyer, 2001).

Reachability means that from each parental state, any other state should be reachable in a finite number of mutations. Mutation operator should be completely unbiased toward individuals with higher fitness values. Instead, selection operator is biased towards fitter individuals. Scalability means that mutation step size should be tunable in order to adapt to the properties of the fitness landscape.

In general, the new individual, $\tilde{y}$, is generated by mutating the recombinant, y, as shown below:

$$\tilde{y} = y + z$$

To determine z, three different equations may be used:

$$z = \sigma \times (N_1(0,1), \dots, N_D(0,1))$$

This method of mutation is called single component mutation that results in concentric spheres around the parental state y. This operator is easy to use since it has only one endogenous strategy parameter however, in some situations it is beneficial to have a vector of endogenous strategy parameters. For those cases, z is determined using the equation below:

$$z = (\sigma_1 \times N_1(0,1), \dots, \sigma_D \times N_D(0,1))$$

This equation results in ellipsoidal surfaces around the parental state y.

In the most general case, when the ellipsoid needs to be arbitrary rotated in the search space, the following should be used to determine z.

$$z = M(\sigma_1 \times N_1(0,1), \dots, \sigma_D \times N_D(0,1))'$$

Where M is an orthogonal rotation matrix. This matrix introduces correlations between the components of z.

3.2.3 **Selection**

The selection operator $a_{m;q}$ takes the m^{th} best individuals out of a population of size q. There are two variations of selection based on using "plus" or "comma" strategies. In case of using "plus" strategy, after generating λ descendants out of μ parents, the best μ are selected among $\mu+\lambda$ individuals. In case of "comma" strategy, after generating the λ descendants, the best μ are selected among the λ descendants.

3.3 Approximate Dynamic Programming (ADP)

ADP was also selected as a method to solve the problem of finding the optimal signal timings in an urban traffic networks with oversaturated conditions over a fixed time period. The ADP algorithm moves forward in time to improve the value of being in each state, which then are used as a decision-making tool. This idea contrasts with that from exact dynamic programming, where the precise value of a state is computed by starting from the last time

period and sequentially backing up in time, building the optimum set of actions toward the starting point. Similar to the standard dynamic programming, the objective of the problem with ADP should be finding (for the whole study period) the argmax of the right hand side of the optimality equation below:

$$V_t(S_t) = max_{x_t}\left(C_t(S_t, x_t) + \gamma E\left(V_{t+1}(S^M(S_t, x_t))\right)\right)$$

Where V_t is the value of state S_t at time t, C_t is a cost function, x_t is the action at time t, S^M is the transition function that finds S_{t+1}, γ is a discount factor, and E is the expectation.

For our specific traffic control problem, the cost function could be defined based on one or multiple measures of performance. For example, the cost could reflect the delay experienced by motorists at the intersection, the number of vehicles waiting for red, or ultimately any combination of traffic-related factors able to provide a useful measure of the goodness of a state.

ADP uses an approximate value function $\overline{V}_t(S_t)$ that is constantly being updated. This makes the algorithm extremely useful as the estimates are available at any point in time (thus, suitable for real-time control), and allows the use of bootstrapping for closing the gap between approximate estimates and the true value of a state.

Since the optimization expression does not require a model of the dynamics of the system over time, the system moves step by step following a transition function that can be provided by a simulation environment (or incoming real-world data). This transition can be in general expressed by the expression below:

$$S_{t+1} = S^M(S_t, x_t, W_{t+1})$$

From above, the state changes from S_t to S_{t+1} in a transition that starts at time t and ends at $t+1$, and W_{t+1} represents the exogenous (or random) information that influences the transition from state S_t to S_{t+1}, after executing action x_t.

This particular element of the system clearly makes the transition function stochastic and captures the variation from one simulation run to the other. Therefore, the states should be visited multiple times not only to improve the estimate of the state value ($V_t(S_t)$), but also to explore the multiple possible transitioning states S_{t+1} upon visiting state S_t.

3.3.1 **ADP "post-decision" state variable**

As it is widely known in the literature, there are a series of variants to the basic ADP algorithm. For our specific problem, it was decided to adopt an ADP algorithm the uses the "post-decision" state variable, more precisely the formulation described by Powell (2007). This algorithm provides a series of computational advantages over more traditional ADP algorithms, as it is explained below.

The "post-decision" state variable uses the concept of the state of the system immediately after an action is taken. This can be described, in general, with the expression that represents the transition function of our problem:

$$S_{t+1} = S^M(S_t, x_t, W_{t+1})$$

Note that this transition can also be expressed as a sequence of two steps:

The state of the system as soon as the action is taken, but no exogenous information from time t to $t+1$ has been received (in other words, vehicles have not reacted to the signal):

$$S_t^x = S^{M,x}(S_t, x_t)$$

The end of the transition, before the next action is decided, and after the exogenous information was received (this is, after the vehicles have reacted to the signal):

$$S_{t+1} = S^{M,W}(S_t^x, W_{t+1})$$

In a similar way, we can describe the value of a state right after a decision is made, and also after receiving the exogenous information:

The action has been decided and executed, at time $t-1$, the exogenous information (w_t) is received and the future state S_t (the state at time t) becomes known:

$$V_{t-1}^{x}(S_{t-1}^{x}) = E\{V_t(S_t) \mid S_{t-1}^{x}\}$$

A decision is made at time t regarding the best action x_t, considering the cost C_t and the expected future state $V_t^x(S_t^x)$:

$$V_t(S_t) = \max_{x^t}\left(C_t(S_t, X_t) + \gamma V_t^x(S_t^x)\right)$$

The action x_t is decided and executed, at time t, the exogenous information (w_{t+1}) is received, and the expected future state (S_{t+1}) is estimated:

$$V_t^x(S_t^x) = E\{V_{t+1}(S_{t+1}) \mid S_t^x\}$$

Note that the standard optimality equation is obtained by combining the last two equations. However, if the first two equations are combined instead, a new expression using the "post-decision" state variable is obtained as follows:

$$V_{t-1}(S_{t-1}) = E\left\{\max_{x_t}\left(C_t(S_{t-1}, x_t) + V_t(S^M(S_{t-1}, x_t))\right)\right\}$$

This expression is very different from the traditional optimality equation mainly because the expectation is outside of the optimization problem. This provides an important computational advantage and allows the algorithm to provide approximated solutions as the number of iterations increases. It also allows for the use of a forward algorithm so that it is no longer needed to loop through all possible states. However, it is required to approximate the expectation of the value function.

Thus, as long as the states are visited with some frequency, it is possible to have "good enough" estimates for adequate decision making support.

The value function, using the post-decision variable, can be updated using a similar equation as the one used in the traditional update rule for temporal difference learning, as follows:

$$\overline{V}_{t-1}^{n}(S_{t-1}^{n}) = (1-\alpha_{n-1})\overline{V}_{t-1}^{n-1}(S_{t-1}^{n}) + \alpha_{n-1}\hat{v}_t^n$$

Where $\overline{V}_{t-1}^{n}(S_{t-1}^{n})$ is the approximated value of the state S_{t-1}^{n} at iteration *n*, and α is the step size or learning rate. The step size determines the weighted value of the current direction pointed out by $\hat{v}_t^n$ in relation to the approximation of the state value at the current iteration.

For convergence to be achieved, the learning rate should decrease over time. These rules require: 1) the step sizes to be non-negative, 2) that the infinite sum of step sizes must be infinite, and 3) that the sum of the square of the step sizes must be finite. These are typical rules for convergence of stochastic gradient algorithms.

It is noted that since it is necessary to have a value of $\overline{V}_t^{n}(S_t^n)$ for each state S_t^n, the problems do not reduce their dimensionality when using ADP, but rather reduce the number of computations needed to find an approximate solution.

3.3.2 **State representation**

There are several ways to represent the state of traffic at a signalized intersection. They vary from the number of vehicles in each approach, to the number of vehicles in queue, to the current delay experienced by those drivers. Each of them may have advantages over the others, and it is not easy to clearly identify the most appropriate for all types of evaluations.

However, from past studies, a very common practice is to use the number of vehicles in queue. This was the approach ultimately adopted for this study, thus the state was defined as a multidimensional space with four components (one for each of four queues waiting for the green light): 1) east-west through movement, 2) north-south through movement, 3) east-west left-turn movement, and 4) north-south left-turn movement.

In addition, the state representation included an extra component that described the current state of the signal (indicating the phase that was currently receiving the green indication). This component was important in order to distinguish the pre-decision state variable from the post-decision state variable, as the state will change as soon as the signal

changes (even if drivers have not reacted to it). At times when the signal was transitioning from one phase to the next, either displaying the yellow indication or in the all-red stage, the state would show the next phase receiving the green indication.

Thus, in total, the state was represented by a five-dimensional space: four components describing the number of vehicles in queue for the four movements, and a component showing the current phase with the right of way.

$$S_t = \{Q_{E-W,Through}, Q_{N-S,Through}, Q_{E-W,Left}, Q_{N-S,Left}, Signal\}$$

3.3.3 **Cost function**

The cost function in our problem was defined, for a given intersection, as a combination of the number of vehicles being served by the green light (with positive sign) and the number of vehicles waiting to be served in the remaining approaches (with negative sign). This general formulation is one of many ways to manage the queues at an intersection, and it is based on the idea of serving the longest queues first.

In addition, penalties were defined for situations in which the size of the queues reached a length close to the capacity of the links. These penalties were designed to prevent queue overflows and de-facto reds, both of which are critical in oversaturated conditions. A second set of penalties was also assigned every time the right of way was switched from one phase to a different one. This accounted for the lost time derived from changing phases, and also prevented the phases to be terminated before they reached a minimum green time that was operationally adequate (say, at least 6 seconds). The general form of the expression to estimate the cost of an action is shown below:

Cost(Phase) = Queue receiving green – Σ (Queue receiving red) + (I(Phase) * Penalty)

Where *I(Phase)* is an indicator function that is equal to 1 if the phase is different from the current phase and 0 otherwise, and *Penalty* is calculated based on an expression of the following form:

$$Penalty = \beta_1 \left(\frac{PhaseDuration + \beta_2}{PhaseDuration - \beta_3} \right) \left(-Q_1\phi_1 - Q_2\phi_2 - Q_3\phi_3 \right)$$

Where β_i are positive coefficients, Q_i is the queue of approach $i \in \{1,2,3,4\}$ such that i does not have the right of way, and ϕ_i is the proportion of the demand in approach i with respect to the total volume arriving at the intersection. Thus, the penalty for changing a phase decreased as the duration of the current phase increased, and it was proportional to the fraction of the demand waiting to be served.

3.3.4 **Eligibility traces – Making the most of every state change**

Eligibility traces are one of the several well known mechanisms of reinforcement learning. The basic idea is to accelerate learning by having deeper updates, as opposed to only updating the value of the state visited in the last time step. Eligibility traces can also be thought as a combination of concepts to bridge Monte Carlo methods (which always perform a full backup) and the standard temporal difference expression - TD(0) (which backs up only one step in time). The algorithms using eligibility traces are typically represented by the letter λ to indicate the extent of the backups, or TD(λ).

The implementation of eligibility traces is relatively easy and is based on a series of weights that keep track of how much time ago a state was visited. They are updated every time the system is updated in such way that the most recent states will have greater weights, and will be affected in greater proportion by new states (compared to those states visited in older time steps). Thus, a new look-up table should be maintained in order to save the current weight of each state (*e(s)*).

There are multiple algorithms already established (for reinforcement learning), including a Sarsa(λ), standard Q(λ), Watkins' Q(λ) (1992), and Peng's Q(λ) (1996). In this study, a modification of the approach used in Peng's Q(λ) algorithm was adopted for the ADP. The ADP algorithm can be summarized in the steps shown in Figure 3.6.

1) Initialization
   a. $V(s)=0$, for all s
   b. Previous action = 0
   c. Eligibility list size = L (L=20, implemented for the last 20 states)

2) Loop from $t=0$ to $t=T$:
   a. Read current state s_t
   b. Determine optimal action (a_t) based on maximum cost $C(a_t)$ and expected future state $V(s_t)$
   c. Carry out action and find short-term reward r_t
   d. Update elements of eligibility list i':
      i. Update eligibilities:
         1. $e(S_i') = \gamma\lambda e(S_i')$
         2. Update α (step size)
         3. Update $V(S_i') = V(S_i') + (\alpha * e(S_i') * (Vmax - V(s_{t-1}))$
      ii. Update current state:
         1. Update $V(s_t)$ estimate (using standard rule)
         2. $e(S_t)=1$

Figure 3.6. Algorithm for Implementing Eligibility Traces

Note that a modification in the update of the trace (*e(s)*) was introduced, so that states that were visited frequently did not have traces greater than 1, potentially distorting the learning process. This modification is known as eligibility trace with replacement, and consists in "replacing" the trace of the visited state with a value of 1 instead of the typical addition of 1 to its current value.

3.4 Implementation

3.4.1 **Genetic Algorithms**

The signal timing optimization problem is formulated as follows:

$$Max \quad \sum_{t=1}^{T}\sum_{i=1}^{N}\sum_{\varphi=2}^{\phi_{ti}} n_{i\varphi}^{t} - \sum_{t=1}^{T}\sum_{i=1}^{N}\sum_{\varphi=2}^{\phi_{ti}} \delta_{i\varphi}^{t} \cdot q_{i\varphi}^{t}$$

s.t.

$$2 \le \phi_{ti} \le 6 \qquad t = 0,\dots,T; \quad i = 1,2,\dots,N$$

$$gmin_{i\varphi}^{t} \le g_{i\varphi}^{t} \le gmax_{i\varphi}^{t} \qquad t = 0,\dots,T; \quad i = 1,2,\dots,N; \quad \varphi = 1,2,\dots,\phi$$

$$0 \le off_{i\varphi}^{t} \le C_{i}^{t} \qquad t = 0,\dots,T; \quad i = 1,2,\dots,N; \quad \varphi = 1,2,\dots,\phi$$

Where:

T: number of study periods,

N: total number of intersections,

ϕ_{ti}: number of phases at intersection i, at time period t,

$n_{i\varphi}^{t}$: total number of vehicles processed by intersection i, at time period t, in phase φ,

$q_{i\varphi}^{t}$: queue length at intersection i, at time period t, waiting to be served by phase φ, and

$\delta_{i\varphi}^{t}$: penalty weight for queue length at intersection i, at time period t, waiting to be served by phase φ.

We deliberately did not include more constraints that are previously established by Grianna and Benekohal (2005) due to the following two reasons:

1. First we wanted to make sure that the algorithm is capable of finding the near optimal answers on its own without introducing those heuristics and,
2. We wanted to make GA, ES, and ADP is comparable as possible to each other.

In particular, the main idea was to bring the definition of these three methods closer to each other and explore their potential in one of their basic forms. For example, it is noted that the formulation for the fitness function in GA and ES used similar measures as the cost function in ADP, and can be briefly summarized as a value that depends on the number of vehicles processed, or throughput (a positive value), minus the vehicles remaining in queue in the approaches not receiving green (a negative value). Thus, despite the fact that measures of performance such as delay or speed could have been added to the formulations, a simple form was preferred to evaluate the potential of the three methods based on the same parameters.

Three different overloading patterns were used to determine the effects of them on the network performance. These loading patterns are:

1- No overloading
2- 10% overloading
3- 20% overloading

For no overloading case, $\delta_{i\varphi}^{t}$ is assumed to be one regardless of the queue length. This means that the objective function is simply penalized by the queue length. For 10% overloading, $\delta_{i\varphi}^{t}$ changes when the queue length in a link changes. However, it is equal to one until the queue fills 10% of the link. Then it is increased as the queue length is increased. Since the length of a left turn link is different than that of a through link, we used different functions for $\delta_{i\varphi}^{t}$ for 10% overloading:

For left lane: $\delta_{i\varphi}^{t}$=$0.013 \times {q_{i\varphi}^{t}}^{2} - 0.0514 \times q_{i\varphi}^{t} + 1.0249$

For Through: $\delta_{i\varphi}^{t} = 0.0032 \times {q_{i\varphi}^{t}}^{2} - 0.0222 \times q_{i\varphi}^{t} + 1.0217$

For 20% overloading the same concept was used. The penalty was constantly equal to 1 until 20% of the link was filled by queued vehicle. Then, $\delta_{i\varphi}^{t}$ was increased according to the following equations:

For left lane: $\delta_{i\varphi}^{t} = 0.000323 \times {q_{i\varphi}^{t}}^{3} + 1$

For Through: $\delta_{i\varphi}^{t} = 0.000033 \times {q_{i\varphi}^{t}}^{3.05} + 1$

A population of candidate solutions is generated to search the feasible area. This population may be generated randomly, or with using some heuristics. Each member of the population, chromosome or individual, is a set of decisions variables that forms a vector. This vector contains signal timing parameters for each intersection, for all defined time intervals. Signal timing parameters for each intersection, in each time interval are phase plan, green time for each phase, and offset. Assuming "*n*" components for this vector, it can be represented as follows:

$$\vec{x} = (x_1, x_2, x_3, \dots, x_{n-1}, x_n) =$$

$$(\emptyset_1^1, g_{1,1}^1, g_{1,2}^1, \dots, g_{1,\emptyset}^1, off_1^1, \emptyset_2^1, g_{2,1}^1, g_{2,2}^1, \dots, g_{2,\emptyset}^1, off_2^1, \dots\dots\dots, \emptyset_{N-1}^1, g_{N-1,1}^1, g_{N-1,2}^1, \dots$$

$$, g_{N-1,\emptyset}^1, off_{N-1}^1, \emptyset_N^1, g_{N,1}^1, g_{N,2}^1, \dots, g_{N,\emptyset}^1, off_N^1;$$

$$\emptyset_1^2, g_{1,1}^2, g_{1,2}^2, \dots, g_{1,\emptyset}^2, off_1^2, \emptyset_2^2, g_{2,1}^2, g_{2,2}^2, \dots, g_{2,\emptyset}^2, off_2^2, \dots\dots\dots, \emptyset_{N-1}^2, g_{N-1,1}^2, g_{N-1,2}^2, \dots$$

$$, g_{N-1,\emptyset}^2, off_{N-1}^2, \emptyset_N^2, g_{N,1}^2, g_{N,2}^2, \dots, g_{N,\emptyset}^2, off_N^2;$$

…

$$\emptyset_1^T, g_{1,1}^T, g_{1,2}^T, \dots, g_{1,\emptyset}^T, off_1^T, \emptyset_2^T, g_{2,1}^T, g_{2,2}^T, \dots, g_{2,\emptyset}^T, off_2^T, \dots \dots \dots, \emptyset_{N-1}^T, g_{N-1,1}^T, g_{N-1,2}^T, \dots$$

$$, g_{N-1,\emptyset}^T, off_{N-1}^T, \emptyset_N^T, g_{N,1}^T, g_{N,2}^T, \dots, g_{N,\emptyset}^T, off_N^T)$$

The decision variable contains the information of all time intervals sequentially. In each time interval, the signal timing parameters of all intersections are present.

The first population is randomly generated and for each individual. Then CORSIM, a widely used microscopic traffic simulation environment, is called to evaluate the fitness value of the first population. Using selection, recombination and crossover, new individuals are generated. This process is continued until enough individuals for the first generation are created. After the new population is generated, the old one is discarded and the process is continued until the termination criteria are met.

3.4.2 **Evolution Strategies**

The problem formulation used in ES is identical to GA as well as the penalties used for queue lengths. To solve the problem with ES, the first population is randomly generated. Each individual contains the signal timing parameters of all intersections in all time periods as well as the endogenous strategy parameters. If we assume that there are "*n"* decision variables, there will be $\frac{n(n-1)}{2}$ endogenous strategy parameters since we use the most general mutation cases to solve the problem . The decision variable is similar to that in GA but has one extra component as shown below:

$$\vec{\boldsymbol{x}} = (x_1, x_2, x_3, \dots, x_{n-1}, x_n, \vec{\boldsymbol{\sigma}})$$

Where $\vec{\boldsymbol{\sigma}} = \left(\sigma_{11}, \ \dots, \sigma_{1n}, \sigma_{21}, \dots, \sigma_{2n}, \dots, \sigma_{n-1,n}, \sigma_{nn}\right)$

After generating the initial population, using recombination and mutation, λ descendants are generated. Then CORSIM is called to evaluate the fitness value of these individuals. In case of "comma" selection strategy the best μ individuals out of these λ parents are chosen. In cases of "plus" strategy, the best μ individuals out of the μ+λ individuals are chosen. This process is continued until the termination criteria are met.

3.4.3 Approximate Dynamic Programming

The microscopic simulation environment provided by VISSIM was used for the implementation of the ADP algorithm. VISSIM provides the option of creating external traffic controllers through its COM interface. This feature was used to read the ADP algorithm, which was coded in C++ and then translated to a dynamic linked library, ready to be used by the simulation in running time.

The state of the system was updated every simulation second, but the controllers perceived it every 2 seconds. This level of detail was able to produce green times with a resolution of 2 seconds. Thus, the system was able to take a decision every two seconds and choose between continuing the current phase and finding a more appropriate phase given the current volume demand, the queue, and phase duration.

For the given network, each intersection was controlled independently by a different external controller (through the COM interface). Therefore, every intersection had its own separate set of state values and learnt the best actions independently. Note that since the system updates were very frequent and in order to maintain the similarity between the parameters between ADP and GA/ES, the exchange of information between intersections was not implemented. As it was defined, the system was able to react within the next 2 seconds of any changes in the queue length. Additional efforts to provide communication capabilities between intersections are expected to provide improvements in performance, mainly for shorter links and lower volume conditions, where coordination may significantly reduce the number of stops and prevent cycle failures.

An additional aspect of the ADP implementation dealt with the state space. Since each of the links could store a large number of vehicles, this could increase the state space to a number difficult to manage. As a result, the actual number of vehicles in queue was scaled down to be represented by a smaller range of queue levels. For the through links (2000 ft long each), vehicles in queue were represented by a number between 0 and 19, and for the left-turn links (1000 ft long each) the scale ranged from 0 to 9. The scaling down was performed by dividing the actual number of vehicles waiting for a given phase by a factor of 6, reducing the resolution of the state representation. Note that two opposing queues will use

the same phase and thus their values will be added to determine the demand for that phase (e.g. eastbound through and westbound through).

As mentioned above, the number of available phases for the controller to choose from was 4, including exclusive left turns and through movements. Therefore, after the queue adjustments (scaling down), the state space for a single intersection was in the order of 202 * 102 * 4 = 1.6×10^5, allowing for the use of standard look-up tables for storing the values of each state ($V(s)$). For future studies and in cases with state spaces that demand more memory, it may be necessary the implementation of function approximation methods instead of look-up tables. A typical approach for such approximations is the use of artificial neural networks.

For the queue estimation, all links in the network were divided into segments of 120 ft, and the vehicles in each segment were considered "queued" based on the following criteria: 1) the speed of the last vehicle entering the segment was below 7mph, and 2) the segment contained more than half of its vehicle capacity. In addition, the queue was required to be continuous, thus once the queue was detected in a given segment of the link, it ended at the first segment where the queue conditions were not met.

The information on the status of the queue was obtained through vehicle detectors placed over the network and allowed the collection of data in real time through the use of the COM interface from VISSIM. However, it is noted that other forms of collecting real-time data through Application Program Interfaces (APIs) are also available, and may also allow the use of other measurements aside from those collected via vehicle detectors.

The implementation of the ADP algorithm did not impose any restrictions on the maximum green times or the phase sequence when finding the optimal actions. The system was allowed to decide exclusively based on the functions and parameters described above, and the ADP was not directed in any way using hard-coded information specific to the tested traffic conditions.

3.4.4 Calibration of VISSIM to CORSIM

As mentioned before our GA and ES are coupled with CORSIM to find near-optimal signal timing parameters. However, ADP is integrated with VISSIM as this package had the flexibility to use external signal controllers that could modify signal timings in real time.

Therefore, to reduce the effects of using different simulation environments, VISSIM was calibrated to CORSIM by taking the following steps:

1- The desired speeds for the two software packages were set to the same value (30 mph)
2- In VISSIM, two different vehicles types were created to match those that are used by default in CORSIM.
3- The additive part of the desired safety distance in the car following model in VISSIM was changed from 2 to 3.9 to match the saturation flow rate and the number of vehicles processed during different green times (5, 15, 25, 35 seconds) in both environments.
4- The standstill distance between the vehicles in VISSIM was changed from 6.9 to 3.9 to match the number of vehicles that could be stored in a link of a given length in both environments.

The resulting conditions allowed the use of the CORSIM solutions (for GA and ES) in the environment provided by VISSIM, and ultimately the comparison of these two methods with ADP.

CHAPTER 4. CASE STUDY

Two networks were used to evaluate the performance of the three selected methods to find near optimal signal timings. The first network was a small hypothetical network while the second was a realistic network created by making some modifications to a portion of the downtown network of the city of Springfield, IL.

The small hypothetical case-study network is symmetric in volume and geometry and composed of nine intersections (a three by three square) that are 2000 ft apart from each other. All streets are assumed to have two lanes (one per direction) and there are exclusive left-turn pockets, 1000 ft in length, at the intersections. We assumed a short study period of 15 minutes in which the traffic demand was fixed with the rate of 1000 vehicle per hour per lane at each entry point. This traffic demand was chosen to be high enough to ensure oversaturation in the network. This case study network is shown in Figure 4.1.

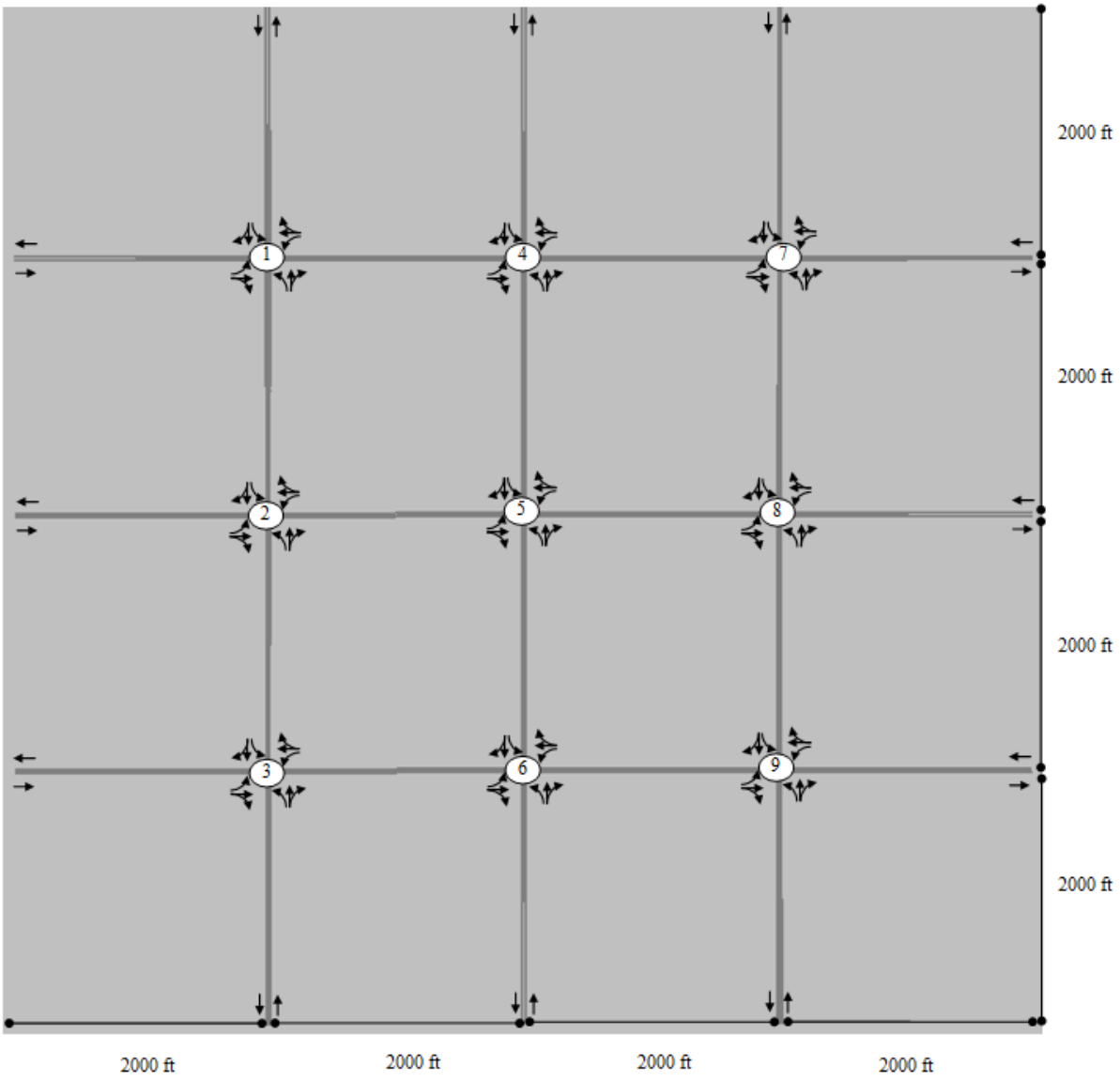

Figure 4.1. Symmetric case study network.

At each intersection the following phase sequence was used for GA and ES. For GA and ES all four phases may used if traffic conditions demand them, otherwise 2 or 3 of the phases may be used. However, ADP did not follow such phase sequence and made the decision to have the left turn phases when the demand justified them.

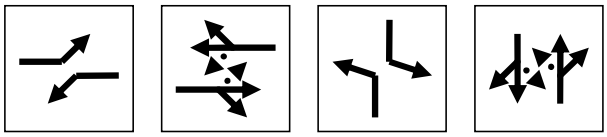

Figure 4.2. Phase Sequence.

In addition to the hypothetical network, a realistic network was used. The main idea in this case was to test the algorithms under a more diverse set of conditions, closer to real world operations. A portion of the downtown network in Springfield, Illinois was used for this purpose. The network in the case study had 20 intersections and a combination of one-way and two-way streets with different number of lanes. It comprised the area between 5th and 11th street from west to east, and between Jefferson and Capitol streets from north to south.

A few modifications were made to the real network in Springfield given the additional vehicular demand used in the test case compared to the actual demand in the field: 1) most of the left-turn lanes in the network were shared, but this was changed by adding exclusive left-turn pockets, 120ft in length; and 2) in cases where there was a lane drop or a lane addition in one of the arterials, the model maintained the same number of lanes along the corridor. The test network is called modified Springfield network, and it is shown in Figure 4.3.

This network did not have protected left turn phases, and as a result, we limited our algorithms to only two phases to control the signals (east-west bound, and north-south bound).

Actual traffic volumes in this part of the network in Springfield are lower than the capacity of links, but the objective of the test case was to examine the network performance in close-to-saturated and oversaturated conditions. Thus, traffic volumes at entry points were increased to match the desired conditions.

We tested two different traffic volumes in the network: 750 vehicles per hour per lane and 1000 vehicles per hour per lane. When traffic volume was 750, we assumed that at all intersections 10% of the drivers made a right turn (when possible), 10% of drivers made a

left turn (when possible), and the rest went through the intersections. When the volume was 1000 vehicle per hour per lane, we assumed that 10% of drivers turned right (when possible), 20% of the drivers turned left (when possible) and the rest went through. It is noted that the turning percentages were estimated as the percentage of incoming volume from a single lane. In other words, the base number to estimate this percentage was the total incoming volume divided by the total number of incoming lanes.

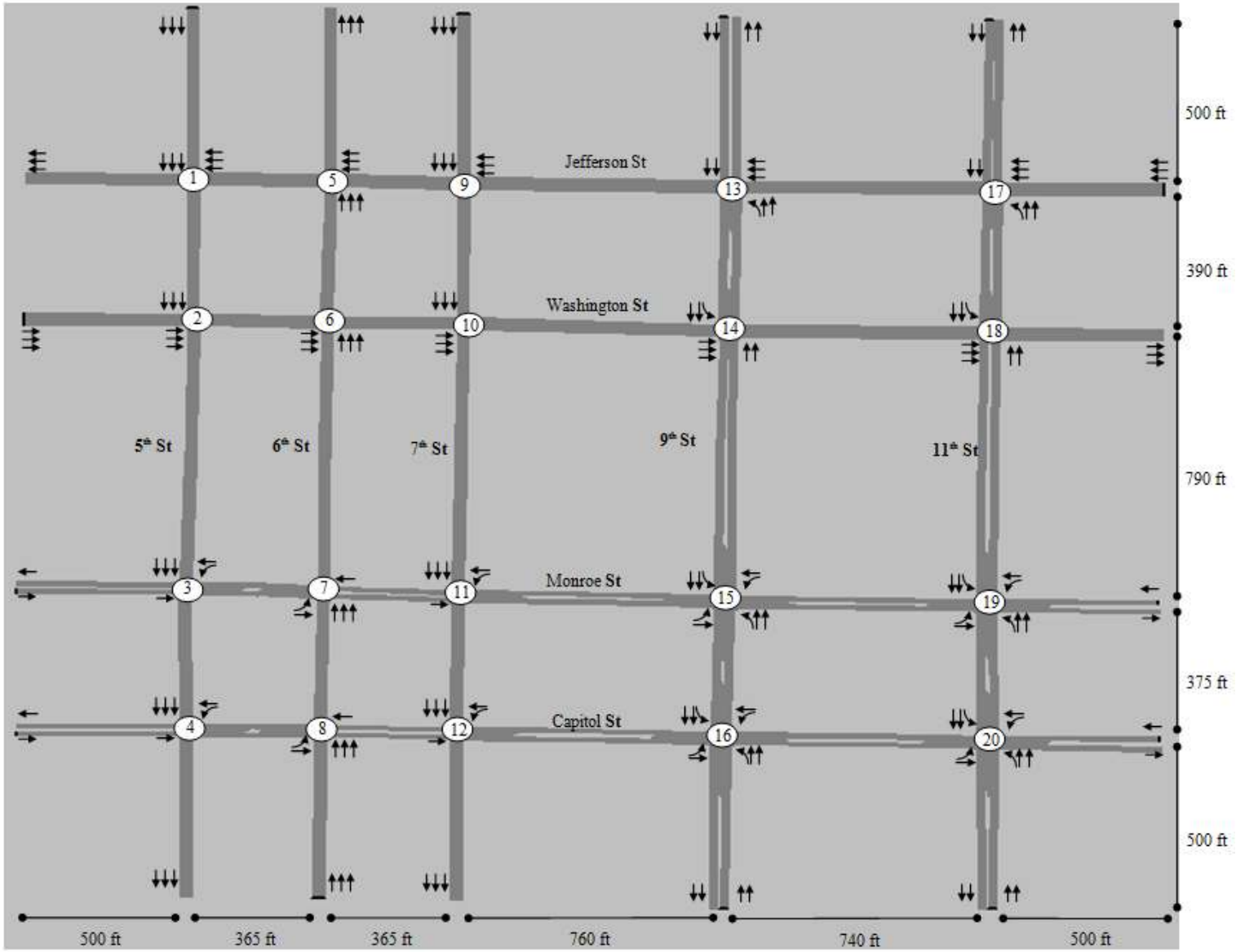

Figure 4.3. Modified Springfield case study network.

CHAPTER 5. SIGNAL TIMING METHODOLOGIES USED

Three different methodologies were used to find optimal signal timings for the two networks: 1) Genetic Algorithms (GA), 2) Evolution Strategies (ES), and 3) Approximate Dynamic Programming (ADP). The first two derive from similar principles and aim at a directed random search of the solution space, whereas the latter aims at learning the best actions over time and it is more suitable for real-time decision-making.

This section presents the signal timings obtained using each of the three methodologies for the following three cases:

1) Case 1 - Network of 9 intersections in oversaturated conditions

2) Case 2 – Modified Springfield network operating in close-to-saturation conditions

3) Case 3 – Modified Springfield network operating in oversaturated conditions

For each case 31 replications of VISSIM were made in each methodology. The study period (duration) for each run is 15 minutes.

5.1 Case 1 - Network of 9 intersections in oversaturated conditions

5.1.1 **Genetic algorithms (GA)**

The signal timings obtained from GA for three different levels of network loading are shown in Table 5.1. Note that GA finds signal timings for each intersection in the network, and these timings do not change during the study period.

Table 5.1. Signal Timings from GA for Case 1

Network Loading	Intersection	Green Phase Duration E-W direction (s)		Green Phase Duration N-S direction (s)		Cycle Length (s)*	Time Difference (s)**
		Left-turn	Right-through	Left-turn	Right-through		
No Overloading	1	6	24	6	28	78	0
	2	6	26	6	26	78	74
	3	6	32	6	32	90	0
	4	6	24	6	30	80	4
	5	6	26	6	28	80	68
	6	6	28	6	32	86	16
	7	6	30	6	34	90	66
	8	6	28	6	32	86	0
	9	6	36	6	36	98	20
	Average	**6.0**	**28.2**	**6.0**	**30.9**	**85.1**	
10% Overloading	1	6	52	6	54	132	28
	2	6	46	6	48	120	16
	3	6	46	6	48	120	64
	4	6	32	6	38	96	56
	5	6	42	6	44	112	4
	6	8	40	6	48	116	46
	7	6	44	6	48	118	96
	8	6	40	6	36	102	94
	9	6	52	6	52	130	34
	Average	**6.2**	**43.8**	**6.0**	**46.2**	**116.2**	
20% Overloading	1	6	52	6	54	132	116
	2	6	46	6	42	114	54
	3	6	52	6	50	128	122
	4	6	46	6	52	124	36
	5	8	52	10	52	136	94
	6	6	34	6	36	96	88
	7	6	48	6	48	122	118
	8	6	46	6	42	114	56
	9	6	40	6	38	104	0
	Average	**6.2**	**46.2**	**6.4**	**46.0**	**118.9**	

* Cycle length calculated assuming yellow time=3 seconds, all-red=1 second. Transition from left-turn to through movement did not require all-red

** Time difference indicates the beginning of the first phase of the E-W direction of a signal according to the simulation clock

Although the average cycle length for the 10% and 20% overloading conditions is similar, a comparison of the cycle lengths for individual intersections (between 10% and 20% overloading) reveals that there were large variations in cycle lengths, indicating that the signal timing changed for each intersection depending on the demand.

A summary of the cycle lengths for the three loading conditions is shown in Figure 5.1, where they are ordered in a 3x3 matrix that follows the same intersection arrangement as the small diagram in Table 5.1. For example the upper left cell of the matrix shows the cycle length (in seconds) for intersection 1, the first cell of the second row shows the cycle length

for intersection 2, and so on. This Figure offers a quick view at the cycle lengths of the whole network.

78	80	90
78	80	86
90	86	98

a) No overloading

132	96	118
120	112	102
120	116	130

b) 10% overloading

132	124	122
114	136	114
128	96	104

c) 20% overloading

Figure 5.1. Cycle Lengths (in seconds) from GA for Case 1

Looking at the animation of the network, it was observed that there was only limited signal coordination and this was expected since the distance between the intersections was 2000 ft (long enough to cause platoon dispersion) and there was residual queue at the end of most of the green phases (given the oversaturated conditions). Long links, however, did accommodate long queues without spilling back to the upstream intersection. Thus, the GA optimization resulted in long cycles that reduced the total lost time in the whole study period, without a significant increase in the probability of overflow or gridlock.

5.1.2 **Evolution Strategies (ES)**

Similar to GA, results from the ES method were obtained for three different network loading conditions: 1) no overloading, 2) 10% network overloading, and 3) 20% network overloading. They are shown in detail in Table 5.2.

Signal timings obtained with the ES method were very similar to their correspondent strategy with GA in terms of both cycle lengths and green splits. Also, the distribution of green times for E-W and N-S movements was balanced.

Green splits and consequently cycle lengths for the overloading conditions were very similar to each other, but different than the no-overloading condition. Green times were

longer and ranged between 36 and 54 seconds, but most of the left-turn movements had only 6 seconds.

Table 5.2. Signal Timings from ES for Case 1

Network Loading	Intersection	Green Phase Duration E-W direction (s)		Green Phase Duration N-S direction (s)		Cycle Length (s)*	Time Difference (s)**
		Left-turn	Right-through	Left-turn	Right-through		
No Overloading	1	6	28	6	26	80	2
	2	6	26	6	26	78	80
	3	6	32	6	32	90	0
	4	6	26	6	28	80	8
	5	6	28	6	28	82	68
	6	6	30	6	30	86	18
	7	6	30	6	32	88	70
	8	6	30	6	30	86	2
	9	6	34	6	32	92	18
	Average	**6.0**	**29.3**	**6.0**	**29.3**	**84.7**	
10% Overloading	1	6	52	6	52	130	26
	2	6	46	6	46	118	14
	3	6	46	6	48	120	60
	4	6	36	6	38	100	54
	5	6	44	6	44	114	0
	6	8	44	6	46	118	40
	7	6	46	6	46	118	92
	8	6	40	6	36	102	86
	9	6	52	6	50	128	28
	Average	**6.2**	**45.1**	**6.0**	**45.1**	**116.4**	
20% Overloading	1	6	52	6	54	132	112
	2	6	46	6	44	116	50
	3	6	52	6	50	128	116
	4	6	48	6	50	124	32
	5	8	52	6	52	132	98
	6	6	40	6	38	104	92
	7	6	48	6	48	122	120
	8	6	44	6	44	114	60
	9	6	38	6	40	104	0
	Average	**6.2**	**46.7**	**6.0**	**46.7**	**119.6**	

* Cycle length calculated assuming yellow time=3 seconds, all-red=1 second. Transition from left-turn to through movement did not require
** Time difference indicates the beginning of the first phase of the E-W direction of a signal according to the simulation clock

A general view at the cycle lengths from the ES is shown in Figure 5.2. These matrices follow the same structure described above for Figure 5.1. The cycle lengths of the nine intersections are similar to those from GA.

80	80	88
78	82	86
90	86	92

130	100	118
118	114	102
120	118	128

132	124	122
116	132	114
128	104	104

a) No overloading b) 10% overloading c) 20% overloading

Figure 5.2. Cycle Lengths (in seconds) from ES for Case 1.

Given that cycle lengths and splits from ES were alike to those from GA, the animation showed similar traffic operation conditions as observed with the GA solutions. The same reasons described above for GA also applied to the ES case, and are related to the long distance between the intersections and frequent residual queues.

5.1.3 **Approximate Dynamic Programming (ADP)**

As explained in Chapter 3, the ADP solution generated variable green times and phase sequences. Results showed that these green times and phase sequences were very similar over time, with some variations depending on the exact arrival pattern of vehicles. This was expected given the constant demand at the entry links and also showed consistency in the performance of the algorithm.

The duration of the green phases and the number of times they were displayed in the 15-minute analysis period are shown in Table 5.3 for the ADP method with and without eligibility traces. Note that the intersections are numbered according to the diagram on the lower right corner of the figure, and the rows are shaded based on the intersection position in the network: a) at the corner – dark shade, b) at the edge, but not at corner – light shade, and c) centered inside the network – no shade. Given the symmetry of the vehicle inputs, it was expected that signal timings for the rows with the same shade (a, b, or c) were similar.

Table 5.3. Signal Timings from ADP with and without Eligibility Traces for Case 1

Intersection	Direction	Phase	No Eligibility				Eligibility			
			Frequency (in 15 minutes)	Green Phase Duration (s)			Frequency (in 15 minutes)	Green Phase Duration (s)		
				Average	Max	Min		Average	Max	Min
1	E-W	Left-turn	4	18	16	2	4	18	16	2
		Right-through	12	27	30	8	11	28	30	8
	N-S	Left-turn	4	18	26	2	4	18	26	2
		Right-through	12	27	38	8	12	28	38	8
2	E-W	Left-turn	5	17	18	6	5	17	18	6
		Right-through	13	25	28	11	13	25	28	11
	N-S	Left-turn	5	16	22	6	5	16	22	6
		Right-through	13	23	32	8	13	23	32	8
3	E-W	Left-turn	4	17	18	6	4	18	18	6
		Right-through	12	27	30	7	12	27	30	7
	N-S	Left-turn	4	19	26	6	4	19	26	6
		Right-through	12	27	32	12	12	26	32	12
4	E-W	Left-turn	4	16	14	2	5	16	14	2
		Right-through	13	24	32	6	13	24	32	6
	N-S	Left-turn	5	17	18	4	5	17	18	4
		Right-through	13	24	48	3	12	25	48	3
5	E-W	Left-turn	5	15	14	4	5	15	14	4
		Right-through	14	21	34	6	14	21	34	6
	N-S	Left-turn	5	15	14	2	5	15	14	2
		Right-through	15	20	26	6	14	22	26	6
6	E-W	Left-turn	5	16	20	6	5	16	20	6
		Right-through	13	23	28	11	12	24	28	11
	N-S	Left-turn	5	16	10	4	5	16	10	4
		Right-through	13	24	36	7	13	25	36	7
7	E-W	Left-turn	4	20	14	6	4	20	14	6
		Right-through	12	27	32	10	11	28	32	10
	N-S	Left-turn	4	19	14	6	4	20	14	6
		Right-through	11	27	32	14	11	28	32	14
8	E-W	Left-turn	5	15	10	4	5	16	10	4
		Right-through	13	24	32	6	13	25	32	6
	N-S	Left-turn	5	15	20	4	4	16	20	4
		Right-through	13	23	34	6	13	24	34	6
9	E-W	Left-turn	4	17	14	6	4	19	14	6
		Right-through	12	26	30	8	12	27	30	8
	N-S	Left-turn	5	18	12	6	4	19	12	6
		Right-through	12	26	32	17	12	27	32	17

= Intersection at edge - CORNER (2 entry links)
= Intersection at edge - NOT corner (1 entry link)
= Intersection on center of network (no entry links)

A series of observations from Table 5.3 are described next. First, the duration and frequencies of phases at intersections in the same group (with the same shade) were very consistent. For example, for the no-eligibility case, the average duration of the right-through phases (for both E-W and N-S directions) at intersections on the corners of the network

ranged between 26 s and 27 s, and each of them were displayed between 11 and 12 times in the 15-minute analysis period. Similar observations are true for the eligibility case, and also for the left-turn movements.

Second, the proportional amount of time allocated to the left turn phases was very close to the actual ratio of demands. For example, the ratio of the total green time for left-turn movements (calculated as frequency * average phase duration) to the total green time for a given direction (e.g. E-W or N-S) ranged between 0.19 and 0.21, when the actual demand ratio was 0.2. This was true for all intersections in both the eligibility and the no-eligibility cases.

Third, the duration of phases with higher number of entry links (which had higher demands) was longer than those with lower number of entry links. This was also expected as the lost time is reduced with longer green times, resulting in a better queue management at the entry links. Also, shorter phases at intersection with lower demand are expected to result in lower delays and better queue management.

Fourth, the frequencies of right-through phases were about three times higher than the frequency of the left-turn phases. This indicates that in practice, the strategy suggests skipping the left turns every two cycles. Considering that the time allocated to the movements is adequate, this solution has the potential to reduce lost time and manage adequately the queue lengths.

Fifth, there is still plenty of opportunities for improvements in the solution since at some cycles the green times were too short (in the order of 2 to 4 seconds), which is unacceptable in practice. An easy fix to this problem can be applied by constraining the green times to a minimum value, but for the purposes of exploring the decision-making of the algorithms, there were no constraints in the process.

In summary, results from ADP suggest that green times for the left-turn movements are about 2/3 of the green times for through movements, but the frequencies of the left turn phases that are about 1/3 of the frequencies the through movement phases. This resulted in a correct allocation of green times, but requires the controller to skip the left-turn phase in some cycles.

5.1.4 Modified ADP – Approximating ADP signal timings to fixed cycles and splits

Cycle lengths or green times were not fixed when ADP is used (with or without eligibility traces). The ADP results were used to find approximate values that resemble fixed time signal operations. The signal timings resulted from this approximation is called Modified ADP. This allowed for direct comparisons of the results based on the Modified ADP with GA and ES results. It also provided solutions that could be implemented in the field with standard traffic controllers. The fixed green times and cycle lengths based on the solutions provided by ADP (without eligibility traces) were estimated using three different approaches, as described next:

1) **Modification 1**: Left turn phases were displayed in all cycles. Green times for through movements were based on averages from ADP. Green times for left-turn phases were estimated from those found in ADP assuming that they will be displayed in all cycles. This resulted in green times as low as 5 seconds in some cases. When the estimated left turn greens were below 7 seconds, all green times were multiplied by a factor that increased the minimum left-turn green time to 7 seconds.
2) **Modification 2**: Similar to Modification 1, but instead of multiplying all green times by a factor, they were added the amount needed to increase the minimum left-turn green time to 7 seconds.
3) **Modification 3**: This approximation did not assume that the left-turn phases will be displayed in every cycle. It considered the frequency of displaying the left turn phases. Green times for through movements were based on averages from ADP.

The exact splits and cycle times for the three ADP modifications are shown in Figure 5.3. There are several key observations to note about the signal timings found in all ADP approximations:

1) The cycle lengths within each of the three ADP modifications are very consistent with each other.
2) They follow the same symmetry of the traffic inputs, so that signal timings of the intersections at the corners are similar (intersections number 1, 3, 7, and 9), intersections with only one entry link are also similar (intersections number 2, 4,

6, and 8), and the timings of the intersection centered in the network (intersection #5) have shorter cycles and splits.

3) The splits for the two competing directions of traffic (E-W and N-S) are balanced. This is according to actual traffic demands.
4) The ratio of splits for the left-turn and the through movements are according to the actual demand ratios (80/20 for through/left traffic).

On the other hand, the three solutions differed significantly in terms of the total cycle length and duration of the splits, as shown in Figure 5.3, and are analyzed in the next section.

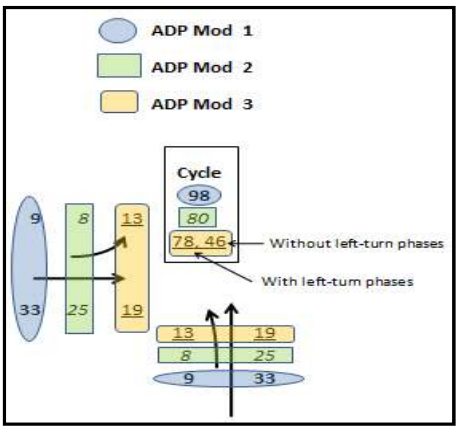

Explanatory key for splits and cycle lengths in part b)

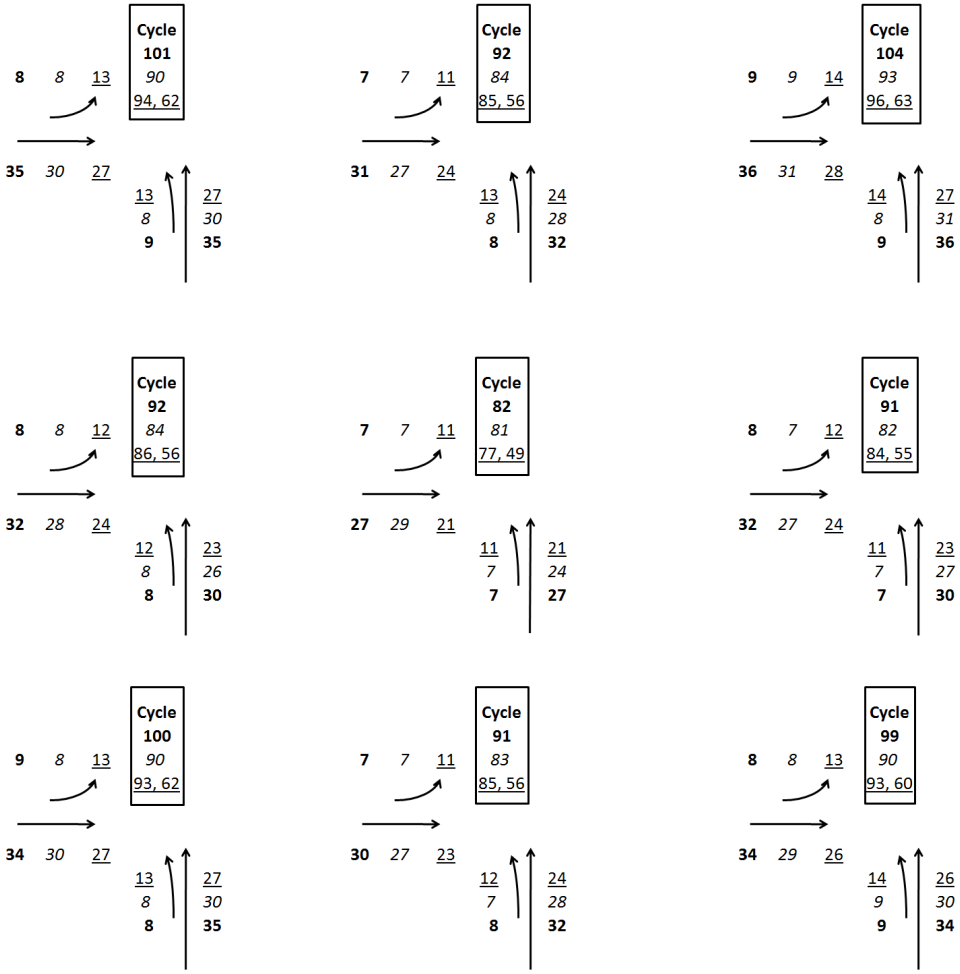

Green splits and cycle lengths for ADP modifications

Figure 5.3. Signal Timings from ADP Modifications for Case 1

In a similar way that it was described for the GA and ES solutions, the cycle length of the intersections from the three ADP modifications are summarized in Figure 5.4 below. Note that the cycle lengths for the ADP modification 3 refer to the cycles that displayed the two left-turn phases, not the cycles without the phases.

101	92	104
92	82	91
100	91	99

a) ADP Modification 1

90	84	93
84	81	82
90	83	90

b) ADP Modification 2

94	85	96
86	77	84
93	85	93

c) ADP Modification 3

Figure 5.4. Cycle Lengths (in seconds) for Modified ADP Solutions in Case 1.

It is also observed that the cycle lengths follow a similar trend to that observed for the original ADP results, with longer cycles for the intersections at the corners of the network (with 2 entry links), followed by the rest of the intersections along the borders of the network (1 entry link each), and the shortest cycle for the intersection located at the center.

5.2 Case 2 - Modified Springfield network in close-to-saturation conditions

The modified Springfield network, with more realistic and diverse settings, was also used to determine the performance of the three methods. Case 2 represents volume levels near saturation at some of the entry nodes (volumes is 750 vphpl). Recall that a two-phase signal was used for all nodes and left turns were permitted from the left-turn pockets during the solid green phase. The signal timings for such conditions are described next.

5.2.1 **Genetic algorithms (GA)**

GA found signal timings with almost identical cycle lengths and even signal time distribution for E-W and N-S direction, as shown in Table 5.4. All cycle length were 72 seconds long except at five nodes (where they either were 2 or 4 seconds greater), and green times were predominantly 32 seconds long, also with a few exceptions (34 or 36 seconds long).

Table 5.4. Signal Timings from GA for Case 2

Strategy	Intersection	Green Phase Duration (s)		Cycle Length (s)*	Time Difference (s) **
		E-W Direction	N-S Direction		
GA	1	32	32	72	24
	2	32	32	72	40
	3	32	32	72	64
	4	32	32	72	0
	5	32	32	72	6
	6	32	32	72	64
	7	32	32	72	64
	8	32	32	72	64
	9	32	32	72	64
	10	32	32	72	4
	11	32	32	72	64
	12	32	32	72	68
	13	34	32	74	16
	14	32	36	76	66
	15	32	32	72	18
	16	32	34	74	70
	17	32	36	76	66
	18	32	34	74	26
	19	32	32	72	70
	20	32	32	72	66
	Average	**32.1**	**32.6**	**72.7**	

* Cycle length calculated assuming yellow time=3 seconds, all-red=1 second. Transition from left-turn to through movement did not require all-red

** Time difference indicates the beginning of the first phase of the E-W direction of a signal according to the simulation clock

Analysis of the values in the Starting Time of the First Cycle indicated that there was signal coordination between some of the intersections, allowing for good signal progression in some of the corridors. Figure 5.5 shows the corridors in which good progression was found. This figure was created based on both the time differences and the animations from the simulation packages. The segments in which coordination was observed are noted with arrows, indicating at one end (diamond shape) the starting point of the vehicle movement from a stop position, and at the other end (arrow shape) the point where the vehicle cleared the last intersection without the need to stop. The coordinated movements are shown separate for E-W and N-S directions.

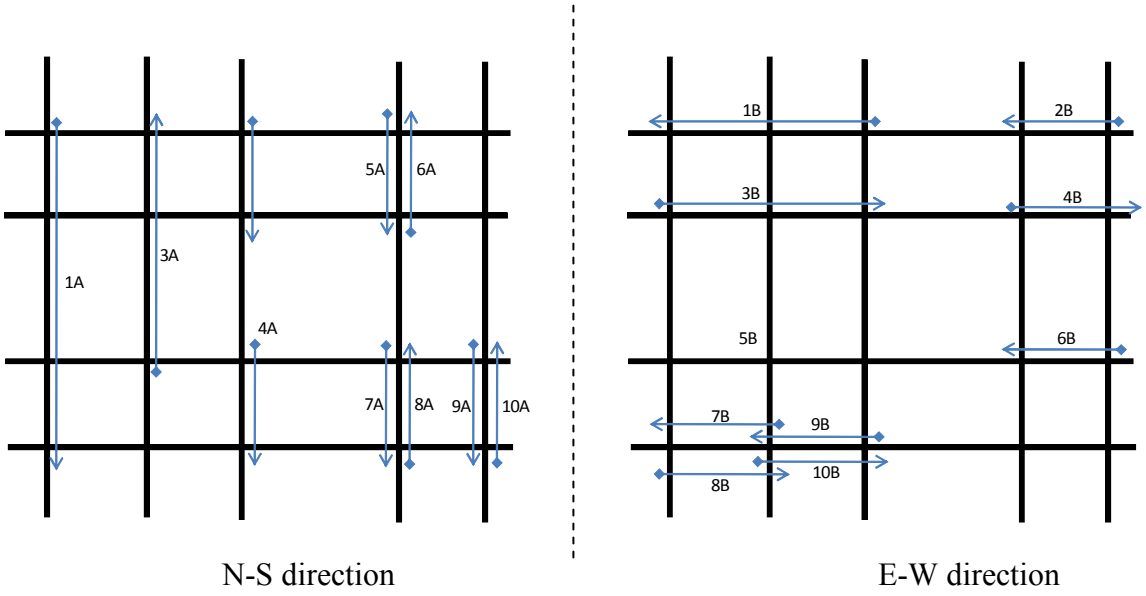

Figure 5.5. Coordination from GA results for Case 2

From Figure 5.5 a few observations are made. The signal timings allowed coordination to some degree in both directions of travel, but did not provide coordination for the entire length of the arterials, except for the corridor shown by arrow 1A. In general, the streets with three lanes (both E-W and N-S) had good progression, with about one stop expected for those within the most favorable bandwidths. Some of the smaller streets also had coordination to some degree, as observed in arrows 5A through 10A and 5B through 10B.

5.2.2 **Evolution strategies (ES)**

Timings from ES were almost identical to those from GA in terms of cycle lengths and duration of green times. Average values at the bottom of tables 5.4 and 5.5 are almost identical, showing that there was also similar distribution of the right of way in the two methods. However, there was more variation in the green times in the ES solution compared to GA, as most of them were not 32 seconds but ranged between 30 and 34 seconds.

Table 5.5. Signal Timings from ES for Case 2

Strategy	Intersection	Green Phase Duration (s)		Cycle Length (s)*	Time Difference (s) **
		E-W Direction	N-S Direction		
ES	1	30	34	72	28
	2	32	32	72	40
	3	30	34	72	68
	4	34	30	72	6
	5	32	32	72	8
	6	34	30	72	70
	7	30	32	70	0
	8	32	32	72	70
	9	32	32	72	70
	10	34	30	72	8
	11	34	30	72	68
	12	32	32	72	68
	13	34	32	74	18
	14	30	34	72	2
	15	30	32	70	0
	16	32	32	72	2
	17	32	34	74	70
	18	32	34	74	32
	19	30	32	70	0
	20	34	32	74	70
	Average	**32.0**	**32.1**	**72.1**	

* Cycle length calculated assuming yellow time=3 seconds, all-red=1 second. Transition from left-turn to through movement did not require all-red

** Time difference indicates the beginning of the first phase of the E-W direction of a signal according to the simulation clock

The offsets in ES were also similar to those from GA, with differences in the order of at most 8 seconds (for intersections 7 and 14) and 18 seconds for intersection 15. This resulted in slightly different coordination patterns, as shown in Figure 5.6. Note that fewer movements are coordinated in comparison with GA, which ultimately resulted in slightly higher delays and number of stops, as it is described in detail in later sections.

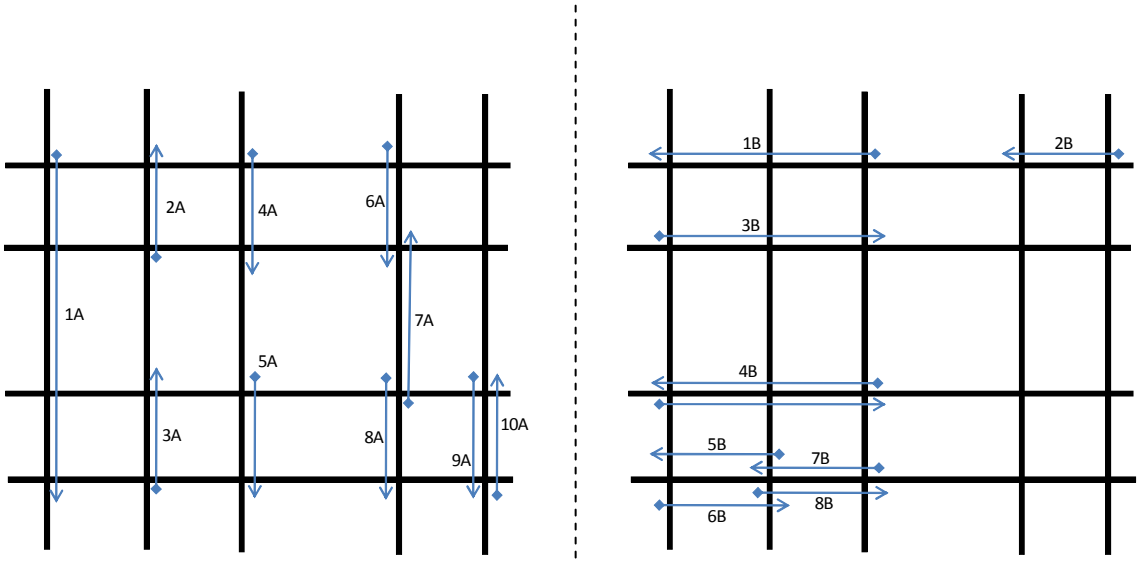

N-S direction E-W direction

Figure 5.6. Coordination from ES results in Case 2

5.2.3 **Approximate dynamic programming (ADP)**

A summary of the signal timings observed with the ADP strategy are shown in Table 5.6. Similar to the results for Case 1, the range of the average green times of the 20 intersections is not very wide (from 16 seconds to 24 seconds), but their maximum and minimum values varied significantly.

The distribution of the green times favored links that carried the entry volume, by providing up to 4 seconds of green time in comparison to the opposing direction of travel. Note that in cases where the opposing traffic was greater than the entry volume, priority was given by ADP to the opposing traffic, as it was the case at intersections 18 and 19.

In comparison to GA and ES, the average green times for ADP are significantly lower, which in turn, resulted in cycle lengths that were about 20 seconds.

Table 5.6. Summary Signal Timings from ADP for Case 2

Intersection	Direction	ADP			
		Green Phase Duration (s)			Phase Frequency (in 15 minutes)
		Average	Max	Min	
1	E-W	16	22	9	21
	N-S	19	23	9	21
2	E-W	18	24	11	21
	N-S	16	22	10	21
3	E-W	19	23	13	20
	N-S	17	22	12	20
4	E-W	19	23	11	20
	N-S	18	24	12	20
5	E-W	18	23	9	21
	N-S	18	22	9	20
6	E-W	17	22	10	21
	N-S	18	22	9	21
7	E-W	19	22	11	20
	N-S	18	23	12	20
8	E-W	18	22	13	20
	N-S	19	23	13	20
9	E-W	17	23	10	21
	N-S	19	24	11	21
10	E-W	18	23	10	21
	N-S	18	23	9	21
11	E-W	19	23	12	20
	N-S	18	23	12	20
12	E-W	19	23	11	20
	N-S	18	23	12	20
13	E-W	19	25	12	18
	N-S	22	36	15	18
14	E-W	18	24	10	19
	N-S	22	51	9	19
15	E-W	18	22	12	21
	N-S	19	23	13	20
16	E-W	18	22	12	20
	N-S	19	23	13	20
17	E-W	17	24	11	21
	N-S	17	23	11	21
18	E-W	17	23	10	21
	N-S	18	25	11	21
19	E-W	18	25	10	18
	N-S	24	42	17	18
20	E-W	17	23	11	21
	N-S	18	23	12	21

5.2.4 **Modified ADP – Approximating ADP signal timings to fixed cycles and splits**

The modified ADP for Case 2 was found by simply using the average duration of the green times as the input for fixed signal timings. Since only two phases were available, and the average green times were not lower than the minimum green time (7 seconds), the options used for Case 1 (modifications 1, 2, and 3) were not needed. The resulting signal timings for modified ADP are shown in Table 5.7.

Table 5.7. Summary Signal Timings from Modified ADP for Case 2

Strategy	Intersection	Green Phase Duration (s)		Cycle Length (s)*
		E-W Direction	N-S Direction	
Mod ADP	1	16	19	43
	2	18	16	42
	3	19	17	44
	4	19	18	45
	5	18	18	44
	6	17	18	43
	7	19	18	45
	8	18	19	45
	9	17	19	44
	10	18	18	44
	11	19	18	45
	12	19	18	45
	13	19	22	49
	14	18	22	48
	15	18	19	45
	16	18	19	45
	17	17	17	42
	18	17	18	43
	19	18	24	50
	20	17	18	43
	Average	**18.0**	**18.8**	**44.7**

* Cycle length calculated assuming yellow time=3 seconds, all-red=1 second.
Transition from left-turn to through movement did not require all-red

5.3 Case 3 - Modified Springfield network in oversaturated conditions

5.3.1 **Genetic algorithms (GA)**

The signal timings obtained with GA for Case 3 are shown in Table 5.8. These settings were significantly different from those found for Case 2 (with lower vehicle

demands). In Case 3, the entering volumes were metered more often with shorter green times, preventing the oversaturation of the links inside the network.

Table 5.8. Signal Timings from GA for Case 3

Strategy	Intersection	Green Phase Duration (s)		Cycle Length (s)*	Time Difference (s) **
		E-W Direction	N-S Direction		
GA	1	24	28	60	4
	2	24	40	72	4
	3	24	40	72	16
	4	24	38	70	66
	5	24	26	58	16
	6	26	24	58	6
	7	26	26	60	4
	8	50	24	82	0
	9	48	24	80	8
	10	26	32	66	0
	11	26	36	70	8
	12	24	38	70	18
	13	40	24	72	8
	14	36	32	76	32
	15	40	32	80	68
	16	48	24	80	16
	17	24	24	56	0
	18	24	24	56	0
	19	24	46	78	64
	20	24	48	80	0
	Average	**30.3**	**31.5**	**69.8**	

* Cycle length calculated assuming yellow time=3 seconds, all-red=1 second. Transition from left-turn to through movement did not require all-red

** Time difference indicates the beginning of the first phase of the E-W direction of a signal according to the simulation clock

In addition, cycle lengths were significantly different from each other (unlike in Case 2). Signal coordination was found only at a few locations, as it is observed in Figure 5.7.

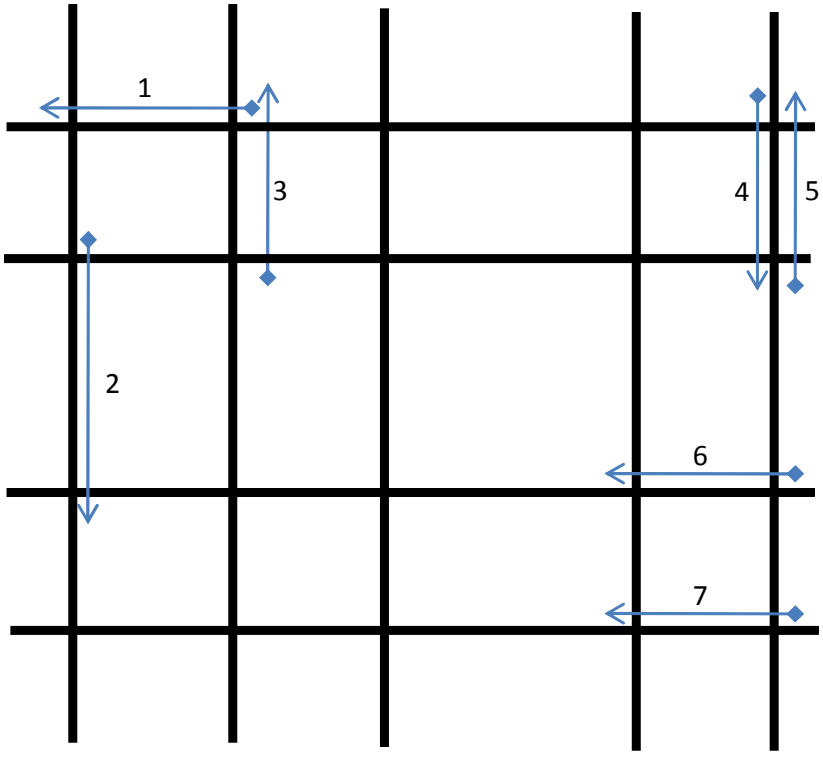

Figure 5.7. Coordination from GA results in Case 3

5.3.2 **Evolution strategies (ES)**

Signal timings from ES are described in Table 5.9. The cycle lengths were shorter for Case 3 compared to Case 2, following the same trends found in the GA solution. On the average, there was an even distribution of green times for E-W and N-S directions, but the green times varied significantly between the two opposing direction of the same intersection, favoring some movements over the others. Most notably, one-way corridors with three lanes were favored over the others, which resulted in green times for such movements that almost doubled the opposing direction. This was the case for the two upper corridors in the E-W direction, and the west-most corridor in the N-S direction.

Table 5.9. Signal Timings from ES for Case 3

Strategy	Intersection	Green Phase Duration (s)		Cycle Length (s)*	Time Difference (s) **
		E-W Direction	N-S Direction		
ES	1	22	22	52	20
	2	22	42	72	0
	3	22	42	72	0
	4	22	34	64	0
	5	22	26	56	20
	6	26	22	56	4
	7	26	26	60	4
	8	48	22	78	0
	9	38	22	68	18
	10	22	30	60	2
	11	22	28	58	2
	12	28	28	64	26
	13	40	22	70	6
	14	38	30	76	30
	15	40	22	70	10
	16	48	28	84	0
	17	22	22	52	8
	18	22	22	52	4
	19	22	38	68	0
	20	22	46	76	0
	Average	**28.7**	**28.7**	**65.4**	

* Cycle length calculated assuming yellow time=3 seconds, all-red=1 second. Transition from left-turn to through movement did not require all-red

** Time difference indicates the beginning of the first phase of the E-W direction of a signal according to the simulation clock

On the other hand, given that cycle lengths were in most cases not similar to each other, signal timings did not result in a significant number of movements being coordinated. This is shown in Figure 5.8, where the coordinated links are indicated by arrows.

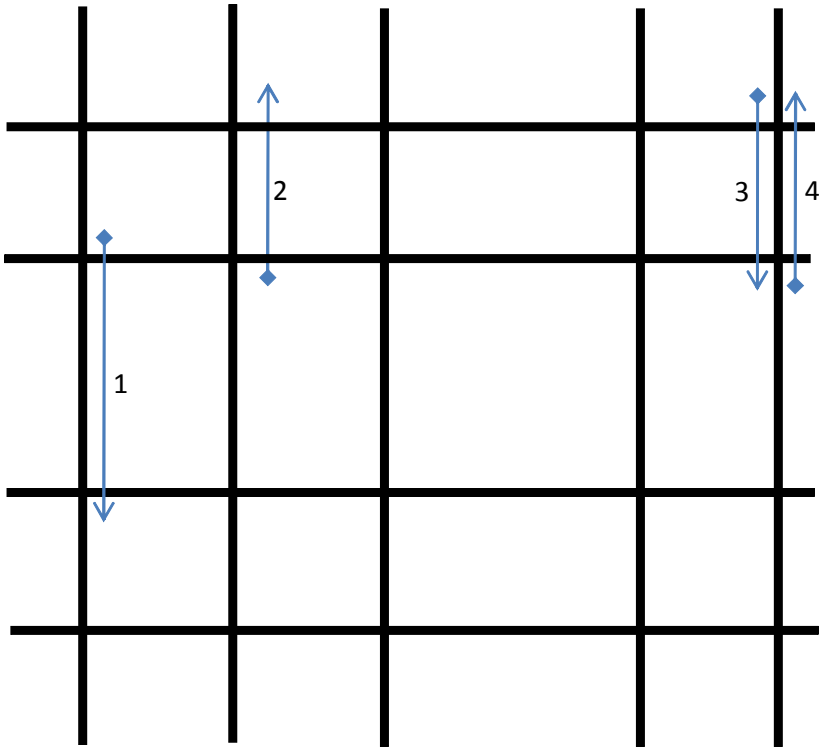

Figure 5.8. Coordination from ES results in Case 3

5.3.3 **Approximate dynamic programming (ADP)**

A summary of the signal timings for ADP for Case 3 are shown in Table 5.10. Average green times were longer than those for Case 2, and in the order of 17 s to 28 s. The maximum and minimum green times had significant variation, with values as low as 6 s and as high as 54 s.

Priorities for green times were not as clear as in Case 2, and some of the arterials carrying greater volume (in particular the three-lane arterials running N-S on the west side of the network) did have in some cases the same or even lower green times than their opposing volumes. This may be the result of greater vehicles metering, which could result in lower probability of blockages due to queue spillbacks. However, some priorities were given to other arterials, mainly to the N-S four-lane two-way arterials on the right side of the network (intersection numbers 13 to 16, and also the stretch from intersection 18 to 20).

Table 5.10. Summary Signal Timings from ADP for Case 3

Intersection	Direction	ADP			
		Green Phase Duration (s)			Phase Frequency (in 15 minutes)
		Average	Max	Min	
1	E-W	19	26	10	20
	N-S	19	37	8	20
2	E-W	19	26	9	19
	N-S	20	36	9	19
3	E-W	23	35	18	17
	N-S	20	32	12	18
4	E-W	21	31	12	19
	N-S	18	24	10	19
5	E-W	18	27	8	20
	N-S	19	28	8	20
6	E-W	19	26	10	21
	N-S	17	25	6	21
7	E-W	19	25	8	19
	N-S	21	39	9	19
8	E-W	22	29	16	18
	N-S	22	37	13	18
9	E-W	22	31	17	17
	N-S	23	40	13	17
10	E-W	18	25	8	20
	N-S	19	29	8	20
11	E-W	21	31	13	18
	N-S	20	33	10	19
12	E-W	19	27	9	20
	N-S	18	28	9	20
13	E-W	21	26	14	16
	N-S	27	46	17	16
14	E-W	20	26	13	16
	N-S	28	53	15	16
15	E-W	20	30	10	18
	N-S	23	40	13	18
16	E-W	21	29	14	17
	N-S	25	41	19	17
17	E-W	22	34	17	17
	N-S	22	30	19	17
18	E-W	18	24	9	19
	N-S	22	38	12	19
19	E-W	21	31	12	16
	N-S	28	54	16	16
20	E-W	21	28	14	16
	N-S	26	42	20	16

5.3.4 **Modified ADP – Approximating ADP signal timings to fixed cycles and splits**

Similar to Case 2, the modified ADP for Case 3 was found by simply using the average duration of the green times as the input for fixed signal timings. Thus for the signal timings for modified ADP, the reader could observed the average values in Table 5.11.

Table 5.7. Summary Signal Timings from Modified ADP in Case 3

Strategy	Intersection	Green Phase Duration (s)		Cycle Length (s)*
		E-W Direction	N-S Direction	
Mod ADP	1	19	19	46
	2	19	20	47
	3	23	20	51
	4	21	18	47
	5	18	19	45
	6	19	17	44
	7	19	21	48
	8	22	22	52
	9	22	23	53
	10	18	19	45
	11	21	20	49
	12	19	18	45
	13	21	27	56
	14	20	28	56
	15	20	23	51
	16	21	25	54
	17	22	22	52
	18	18	22	48
	19	21	28	57
	20	21	26	55
	Average	**20.2**	**21.9**	**50.1**

* Cycle length calculated assuming yellow time=3 seconds, all-red=1 second. Transition from left-turn to through movement did not require all-red

CHAPTER 6. PERFORMANCE OF THE DIFFERENT STRATEGIES

The performance of the networks under various signal timings were compared using a series of measures of performances (MOP) that included traffic-related issues, computational effort, and ease of use. Some of the MOP were focused on the queue lengths and potential queue overflows (causing de-facto red) since the networks were oversaturated.

This chapter is divided into three sections. In the first section the findings of the small oversaturated network are presented. In the next section the results for the modified Springfield network in close-to-saturation condition is presented, followed by a scenario when it is operating in oversaturated condition.

It should be noted that to determine any of the MOP the signal timing parameters found by each method (GA, ES, or ADP) were used as an input to VISSIM with a total study period of 15 minutes. To take the internal variability of VISSIM into account, 31 simulation runs were made and the MOPs presented below reflect the results of those 31 runs.

6.1 Case 1 - Network of 9 intersections in oversaturated conditions

6.1.1 **Average delay and network saturation**

The first MOP that was analyzed was the average delay of all vehicles. A summary of the range of the average delay from the 31 replications for each of the methods is shown in Figure 6.1. It also shows the number of vehicles in the network at the end of the simulation period (as a measure of network congestion).

This analysis included the delay for vehicles that could not enter the network due to long queues in the entry links. This factor was important in comparing solutions from different methods since the inner links with less congestion show lower delay but at the cost

of not allowing vehicles to enter the network. This consideration also works in favor of fairness to all strategies and adds a more realismto the calculations, accounting for metering effects at the edges of the network. Thus, the standard estimation of delay performed by VISSIM (the difference between the ideal travel time -no traffic, no control- and the actual travel time experienced by the drivers) was modified to include the delay of vehicles waiting to enter the network.

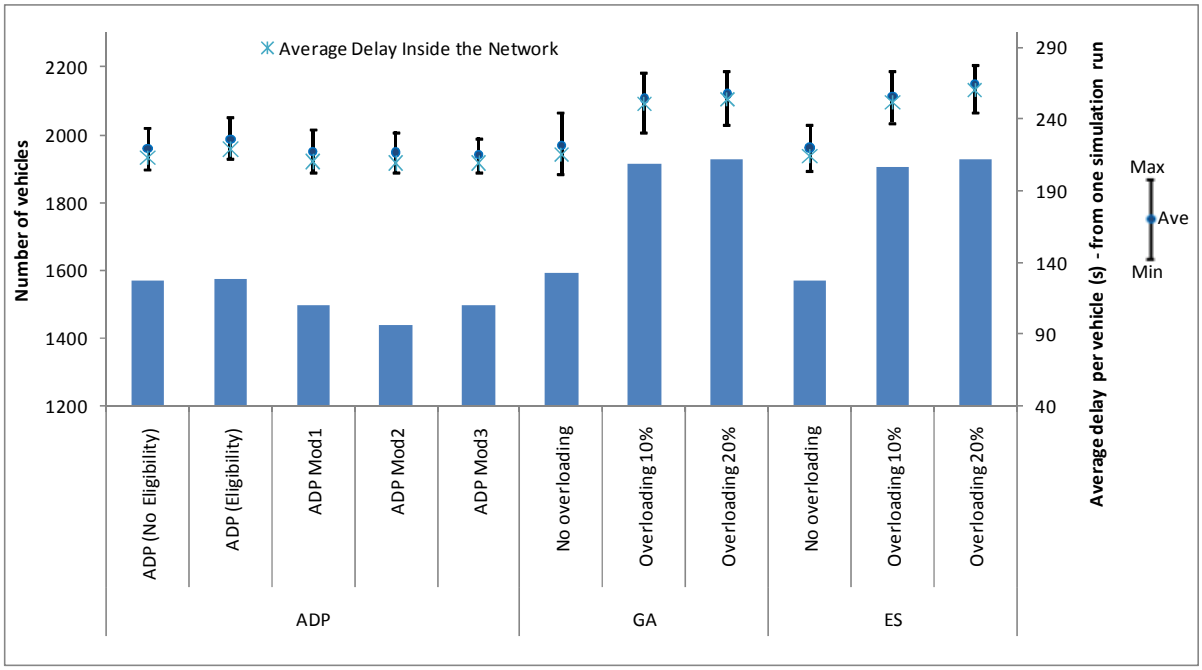

Figure 6.1. Average Delay and Network Congestion for Case 1

Figure 6.1 shows similar delays for the ADP (and its modifications) as well as the GA and ES with no network overloading - with average delays per vehicle around 220 seconds. The performance of the GA and ES algorithms with overloading options was not as favorable, with average delays close to 255 seconds.

The contribution of delay from vehicles outside the network was very low and represented less than 4% of the total delay, as it is shown in Table 6.1. In general, all strategies managed to keep the back of the entry queues in such way that only a few vehicles were delayed outside of the network. The values from Table 6.1 were found by tracking the

queues and the blockage at the entry links, and assuming a constant (expected) arrival rate of one vehicle every 3.6 seconds based on entry volumes (1000 vehicle per hour per lane).

Figure 6.1 also shows that the total delay increased with the number of vehicles in the network at the end of the simulation period, as the bars in the figure follow the same trends as the delay ranges. Thus, as the saturation level of the network increased, the total average delay per vehicle also increased.

These considerations suggest that there should be an optimal level of network saturation in order to achieve low average delays, high throughputs, and good queue management.

Table 6.1. Delay of Vehicles Outside the Network for Case 1

		ADP					GA			ES		
		ADP (No Eligib.)	ADP (Eligibility)	ADP Mod1	ADP Mod2	ADP Mod3	No overloading	Overloading 10%	Overloading 20%	No overloading	Overloading 10%	Overloading 20%
Vehicles delayed outside of the network (at entry points)	Min	174.44	219.24	225.4	281.96	231.84	199.92	101.08	119	194.88	127.96	116.76
	Average	268.0413	292.3	321.9	357.0	304.6	274.6	199.5	200.0	293.1	218.9	227.8
	Max	335.44	375.76	390.6	412.16	366.24	357	274.12	283.64	370.16	292.04	298.76
Cummulative delay (s) of those vehicles delayed prior to enter	Min	8194.48	13509.44	12737	15591	10100	9971.92	4509.12	5650.4	9628.64	6688.08	5486.32
	Average	17359.2	21458.9	21030.9	#######	18464.3	18489.7	10918.2	10816.4	17195.8	12350.0	12616.1
	Max	26326.72	35735.28	30878	34855	26565	37978.64	16252.88	19422.48	25424	17922.24	19791.52
Average Ratio Delay vehicles outside/Total delay		**2.6%**	**3.2%**	**3.2%**	**3.5%**	**2.9%**	**2.8%**	**1.4%**	**1.4%**	**2.6%**	**1.6%**	**1.6%**

6.1.2 **Network throughput**

The network throughput was defined as the total number of trips completed, or in other words, the total number of vehicles that had left the network at the end of the analysis period. A summary of the throughput for all strategies is shown in Figure 6.2.

In general, signal timings that result in a greater number of vehicles completing their trips are more desirable. GA, ES, ADP without eligibility traces and its modifications, as well ADP with eligibility traces, resulted in similar network throughput that ranged from 2220 to 2320 vehicles. It is noted that the expected demand for the 15-minute analysis period was 3000 vehicles, indicating a hard-to-reach upper bound for the number of processed vehicles.

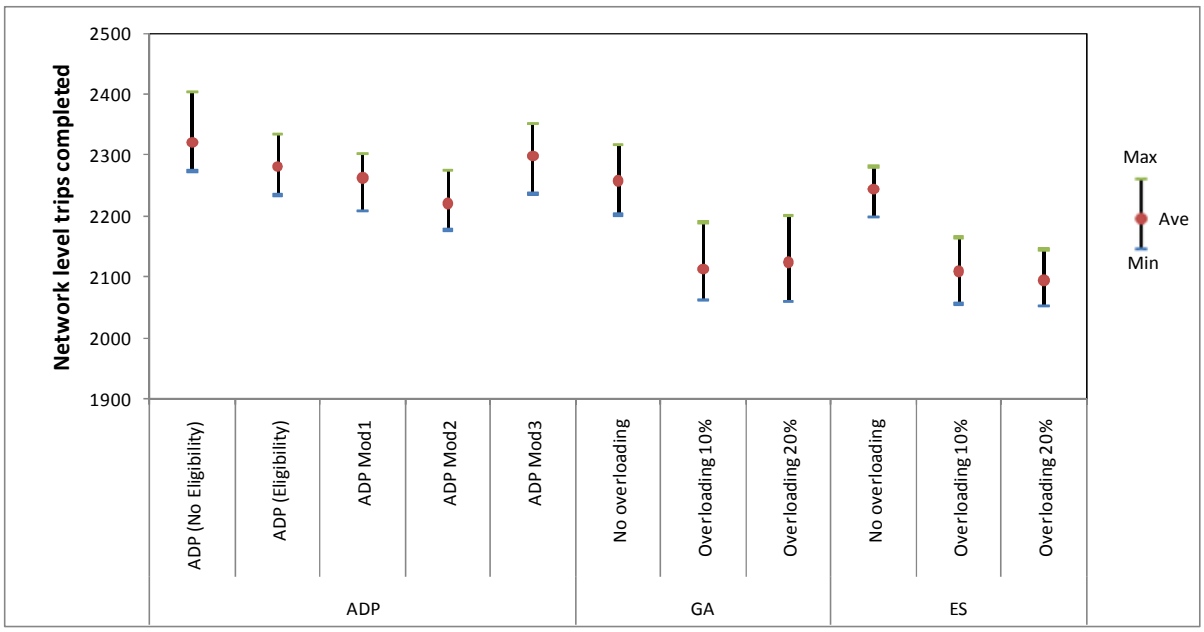

Figure 6.2. Network Throughput (Trips Completed) for Case 1

A closer look at the number of vehicles inside the network revealed that the network increased its saturation levels over time, since the number of vehicles processed was lower than the actual demand. This was expected since the arriving volume at the intersections with two competing entry links (the four intersections at the corners) was about 2000 vph, which exceeds the actual capacity of signalized intersections with single lane approaches.

6.1.3 **Average speeds**

Trends from average speed data were very similar to those from the vehicle throughput, as it can be seen from Figure 6.3. Higher speeds were obtained with the ADP approaches and the GA and ES without network overloading, and they were in the order of 10.3 mph to 10.7 mph. Recall that the desired speed of the drivers in the network was 30 mph. Based on the findings, it is easy to observe that in general lower delays and greater throughput resulted in higher average speeds.

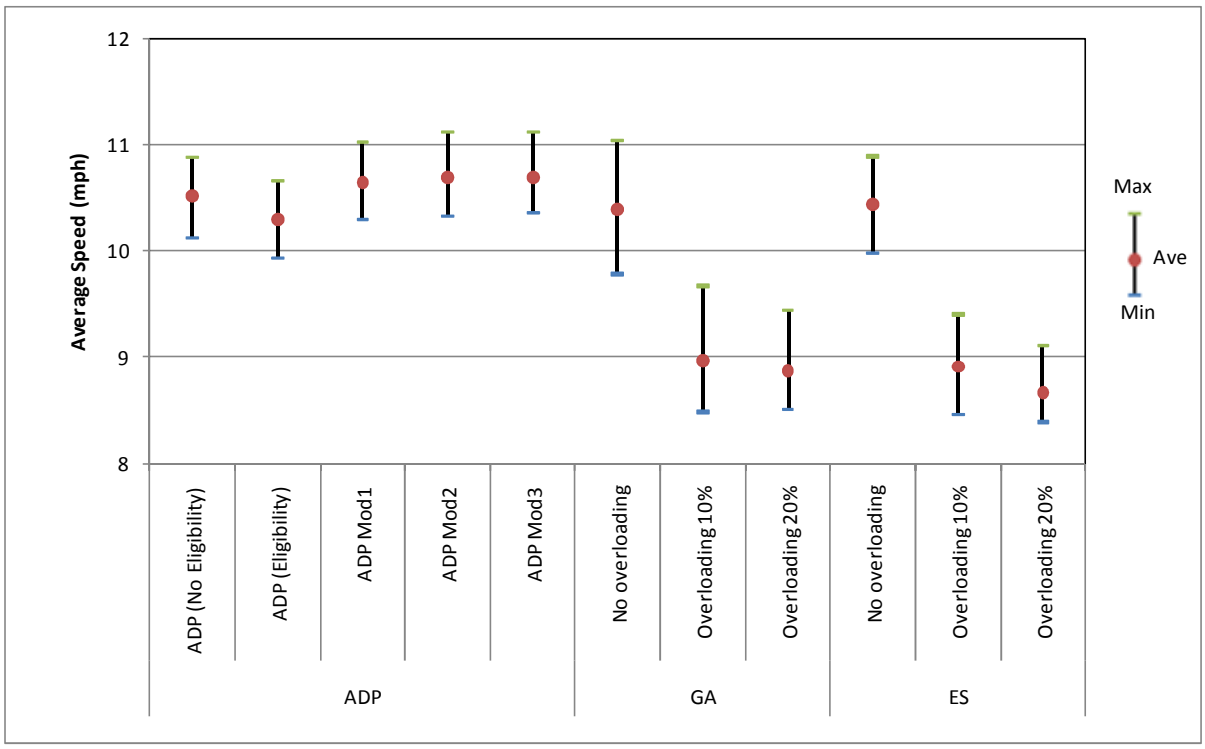

Figure 6.3. Average Vehicle Speeds for Case 1

6.1.4 **Average number of stops and stopped delay**

The average number of stops and the average stopped delay per vehicle, are shown in Figure 6.4. Note that there was an inverse relation between the number of stops and the stopped delay, as expected. This was the case since lower number of stops were obtained when green times were longer, but this also resulted in vehicles having to wait longer for the next cycle to begin - and for an opportunity to speed up again. In fact, the GA and ES solutions with network overloading did result in lower number of stops, but higher delays and lower throughputs than other solutions.

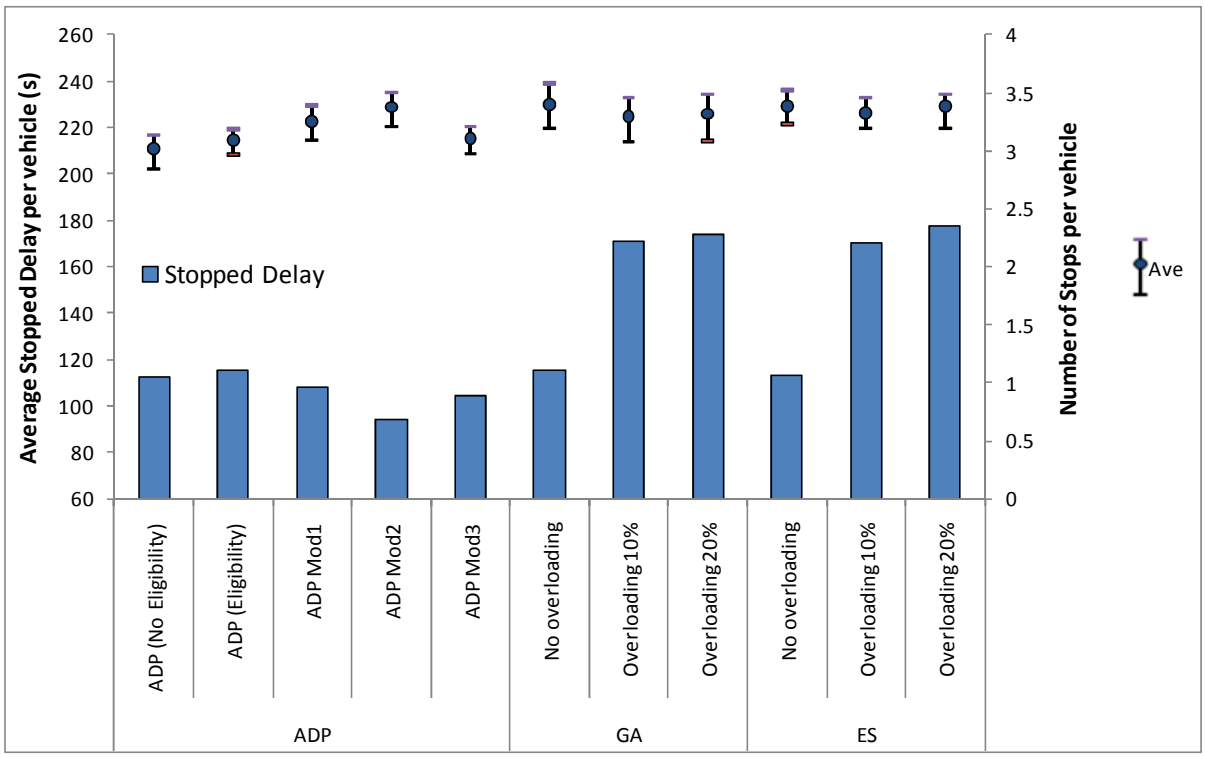

Figure 6.4. Number of Stops and Average Stopped Delay for Case 1

It was also observed that the average stopped delay was directly proportional to the total average delay, thus the ratio of stopped to total delay increased as the stopped delay increased. This is a sign of added congestion in the system (vehicles stopped completely for longer time periods), and it was found mainly in the overloading scenarios from the GA and ES. Details are shown in Figure 6.5, below.

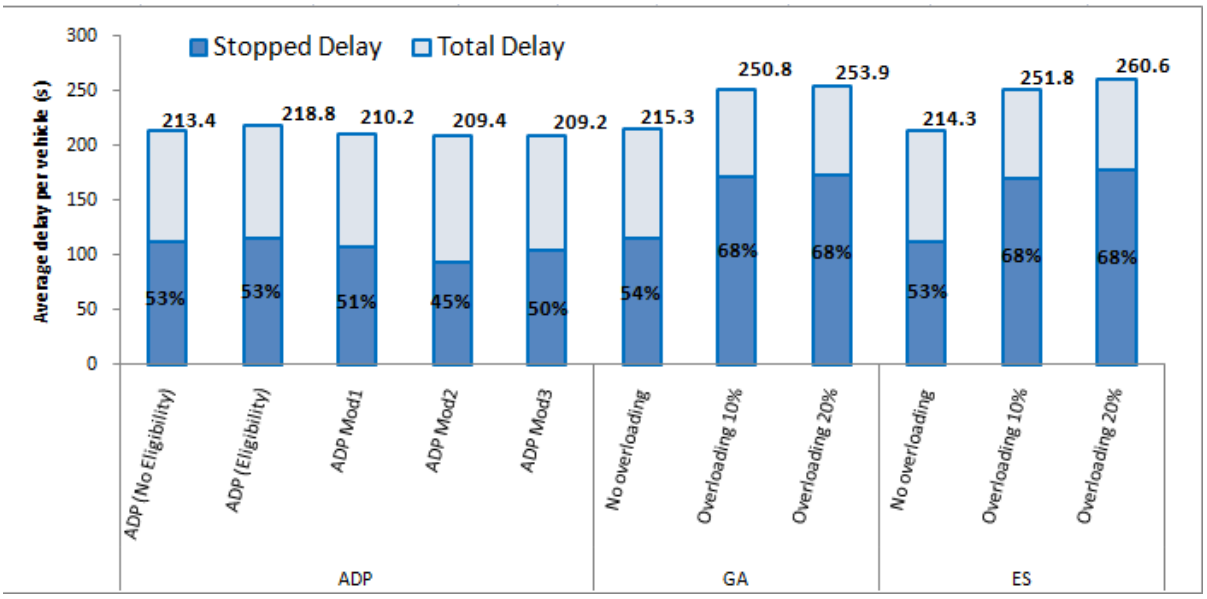

Figure 6.5. Ratio of Stopped Delay to Total Delay for Case 1

Overall, it was found that a better strategy was not to minimize the number of stops, but to minimize the total stopped delay and manage the length of the queues.

6.1.5 **Efficient use of green**

Another sign of good signal timing could be defined in terms of the amount of green time that is not used to process the greatest number of vehicles, in other words, when vehicles do not cross the stop bar at saturation flow. This is likely to be the case when (in oversaturated conditions) the entire queue before the end of the green has been completely discharged.

Therefore, the length of the queue was monitored for entry and non-entry links and for through and left-turn movements, recording the amount of time that the queue was completely dissipated. Results are shown in Figures 6.6 and 6.7.

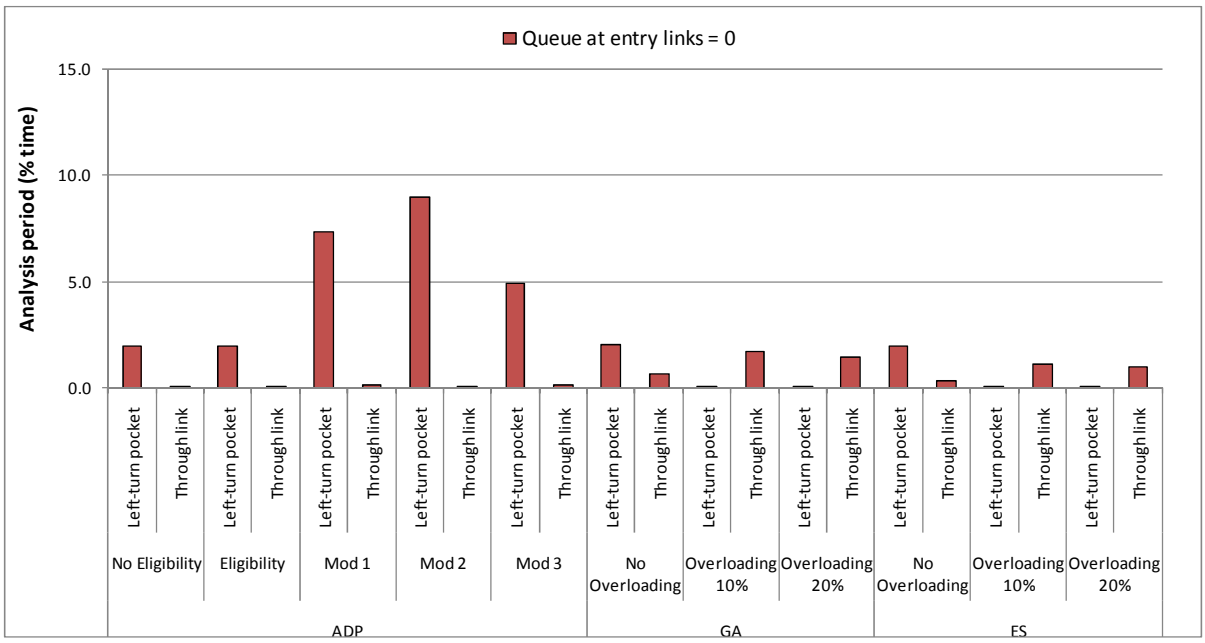

Figure 6.6. Percentage of Time that Queues were Zero at Entry Links for Case 1

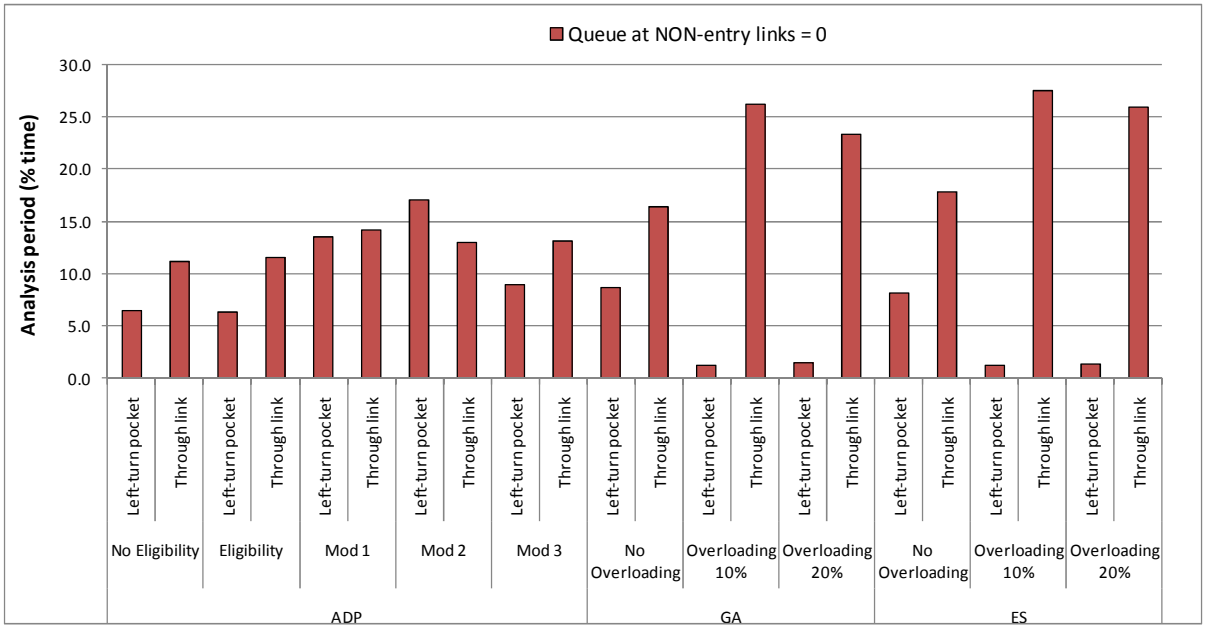

Figure 6.7. Percentage of Time that Queues were Zero at Non-Entry Links for Case 1

In Figures 6.6 and 6.7, lower percentages of queue lengths equal to zero was considered desirable. Note that the ADP strategies (eligibility and no-eligibility) were in

general more efficient at preventing serving approaches with queue equals zero. This is expected since the algorithms adjusted the signal timing settings in real time and not based on average performance, which was the case for the other strategies.

6.1.6 **Queue overflows**

Carefully managing the queues is extremely important in an oversaturated network to ensure a more efficient operation. Particular attention should be given to the back of queues so that queue overflows do not occur. Queue overflow blocks the upstream intersection and prevents vehicles from discharging, creating a "de-facto red" situation. Queue overflows can create a gridlock in the network. A gridlock significantly deteriorates the performance of networks and results in longer delays and lower throughput. The occurrence of queue overflows was monitored for all signal timing solutions, by determining if the back of queue at entry and non-entry links reached the upstream intersections (or the end of the link). Results are shown in Figures 6.8 and 6.9.

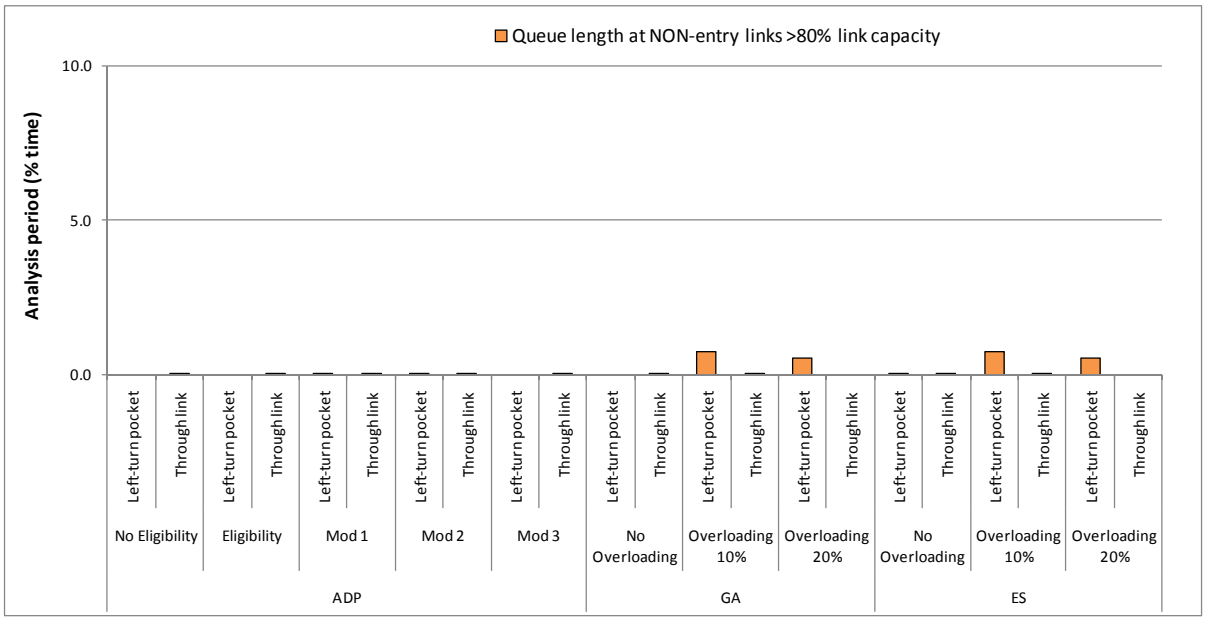

Figure 6.8. Potential Queue Overflows at Non-Entry Links for Case 1

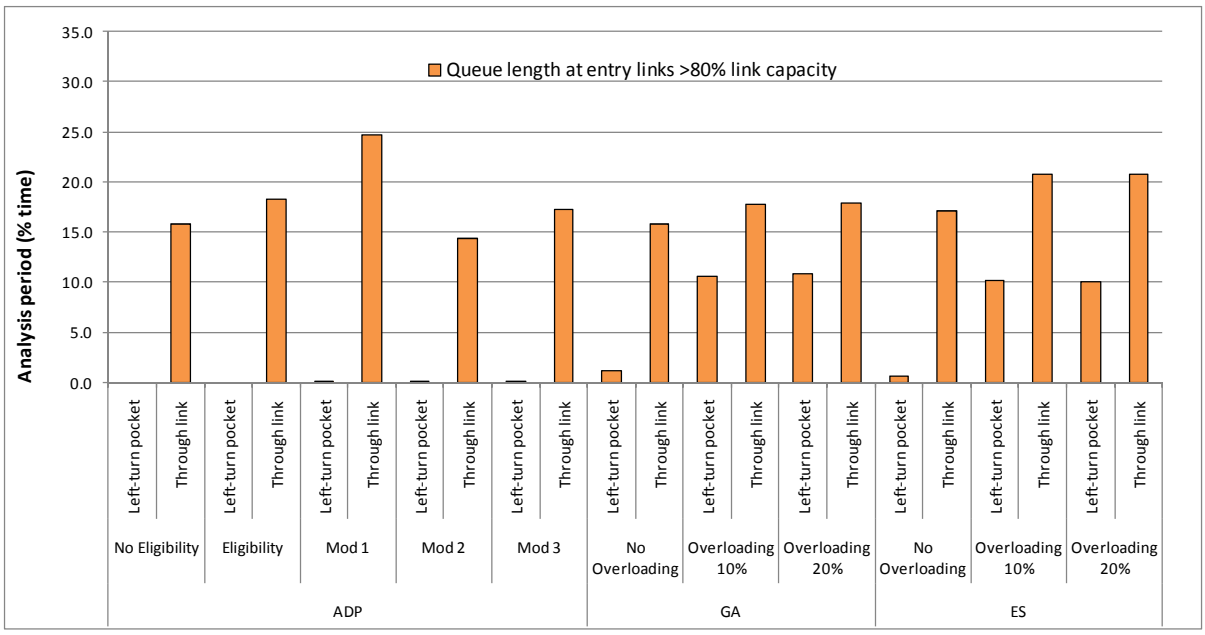

Figure 6.9. Potential Queue Overflows at Entry Links for Case 1

Figure 6.8 shows that signal timings from all three methodologies effectively managed the queues inside the network and prevented queue overflows. However, it was noticed that left-turn queues (and in minor proportion, the through queues) sometimes reached the beginning of the entry to pocket at entry links (Figure 6.9). This may prevent through vehicles from filling up the through link near the stop bar, increasing delays and reducing the effective link capacity. This was the case mostly for the GA and ES solutions with overloading (both 10% and 20% overloading), where an average left turn pocket at the entry links reached more than 80% its capacity for about 15% of the total simulation time. This was expected since network overloading favored a higher number of vehicles in the links.

6.1.7 **Extreme delay values**

In addition to general measures of performance, the extreme values of the delay were also monitored. This analysis reveals the least-favored movements and the amount of delay for vehicles in such routes, as well as potential limitations on the applicability of certain

strategies. Table 2 shows the average, maximum, and minimum number of vehicles with delays (per link) greater than 300 seconds, as well as the maximum delay in a single link, for all strategies.

Table 6.2. Maximum Delays per Link and Vehicles with Delays Greater than 300 Seconds for Case 1

Strategy		Statistic	Max Delay in one link (s)	# of Vehicles with delay >300s in one link
ADP	No Eligibility	Min.	422	94
		Ave.	**513**	**152**
		Max.	664	204
	Eligibility	Min.	451	117
		Ave.	**524**	**171**
		Max.	607	245
	Mod 1	Min.	393	22
		Ave.	**491**	**79**
		Max.	612	166
	Mod 2	Min.	391	31
		Ave.	**499**	**79**
		Max.	670	137
	Mod 3	Min.	372	40
		Ave.	**498**	**109**
		Max.	658	167
GA	No overloading	Min.	527	135
		Ave.	**671**	**231**
		Max.	832	319
	10% overloading	Min.	786	463
		Ave.	**901**	**520**
		Max.	1094	591
	20% overloading	Min.	769	464
		Ave.	**890**	**519**
		Max.	1017	591
ES	No overloading	Min.	531	136
		Ave.	**652**	**219**
		Max.	780	281
	10% overloading	Min.	762	474
		Ave.	**898**	**519**
		Max.	1070	606
	20% overloading	Min.	764	471
		Ave.	**890**	**538**
		Max.	1045	592

From Table 6.2, the best worst-case delays are obtained with the ADP modifications 2 and 3, where it was very rare that a vehicle had delays of more than 300 seconds on a single link. At the other end of the results, the overloading options with GA and ES had the highest maximum delays and number of vehicles with delays greater than 300 seconds, showing very unfavorable conditions for some of the drivers in the network.

It is also important noting that for all strategies, all vehicles that experienced delays greater than 300 seconds were left turners. Thus, all strategies clearly favored through movements as opposed to left turns. This was expected since ratio of the through vehicles to left-turners was 80/20, but in oversaturated conditions it also resulted in delays that seemed (in some cases) very high for real-world applications.

6.2 Case 2 - Modified Springfield network in close-to-saturation conditions

In a similar way that the results were presented for Case 1 (the small network of nine oversaturated intersections) MOEs are also presented in this section for Case 2 in the modified Springfield network. In this case it is assumed that entry volume is 750 vehicles per hour per lane at the entry links. For Case 2, ADP with no eligibility traces, a modified ADP, GA with no overloading, and ES with no overloading were used.

Average delay per vehicle, 10^{th} and 90^{th} percentiles delay, min, max, and the number of vehicles in the network at the end of analysis period are shown in Figure 6.10.

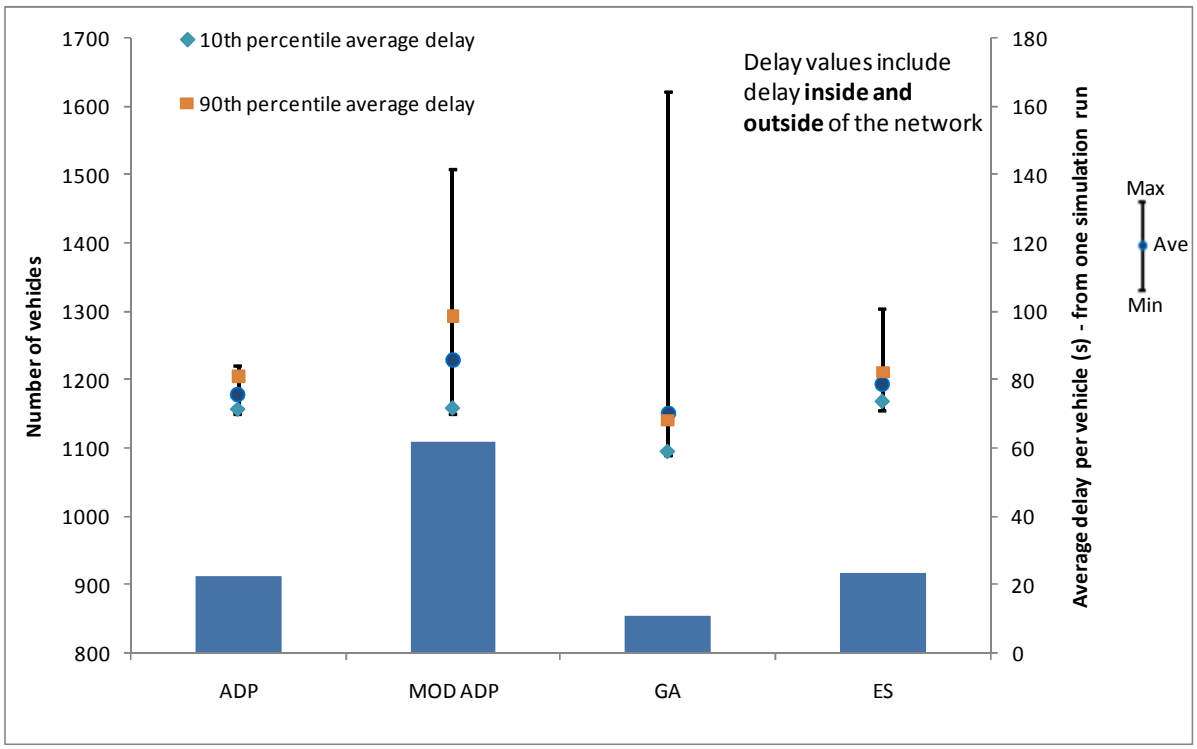

Figure 6.10. Average Delay and Network Congestion for Case 2

Average delays per vehicle were 70s to 85s, being the results from GA the lowest and the results from modified ADP the highest. As presented in the Figure, for GA the range of average delay is extremely wide. However, the 10th and 90th percentiles are very close to each other. In fact, the 90th percentile delay was less than average delay. This was due to three seeds that resulted in extremely long delays that were two times larger than the average delay.

The greatest delay values for GA and modified ADP were the result of intersection blockages due to queue spillbacks, mainly caused by the stochastic nature of the vehicle arrivals. Lower fluctuations were in fact expected for ADP since it could react in real time to these stochasticities, as opposed to fixed timings.

The importance of vehicles delayed outside the network due to queues at the entering links was minimal with respect to the total delay. The higher average value was for GA, with a ratio of outside delay to total delay of 1.7%, and the lowest was for ADP with an average of 0.2%.

In relation to the number of vehicles in the network at the end of the analysis period (see the bars in Figure 6.10), the modified ADP allowed about 20% more vehicles than the other methods (with an average of 1100 vehicles), increasing the network load. This may result in higher probability of queue spillbacks as the signal timings are fixed, but it may also reduce delays outside of the network.

The network throughput in the 15-minute evaluation period is shown in Figure 6.11. Note how the averages for all four methods were very similar, but higher fluctuations were found for modified ADP and GA. This is due to the same stochastic effects that affected the average delays, mentioned above. Similar to average delay, three of the seeds created extremely unfavorable network conditions for GA. Similar to delay, the 10th percentile throughput was greater than the average throughput.

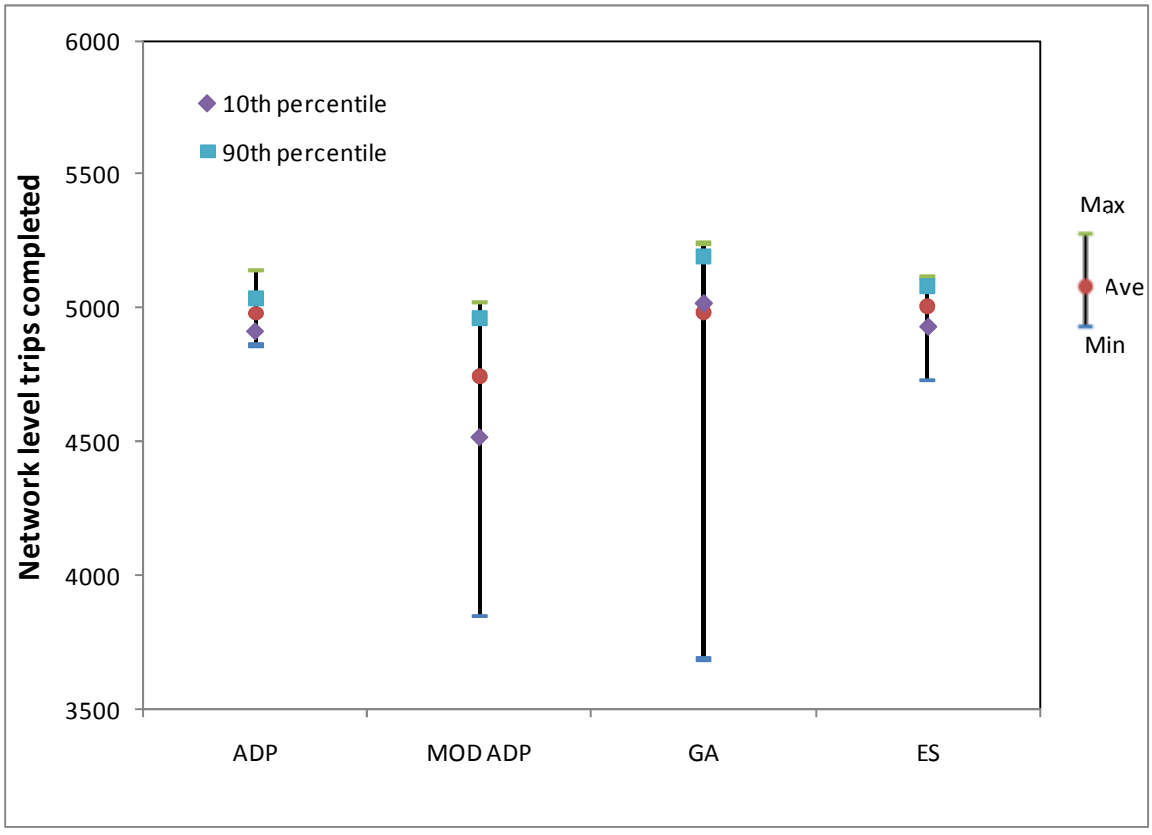

Figure 6.11. Network Throughput (Trips Completed) for Case 2

Note that the upper bound for this value was the number of vehicles in the network after reaching equilibrium (~500 vehicles) plus the actual demand for the study period (totaling 5062 vehicles on average – this number is the result of 750 vphpl per link in 27 entering lanes for 15 minutes), which was in the order of 5500 vehicles.

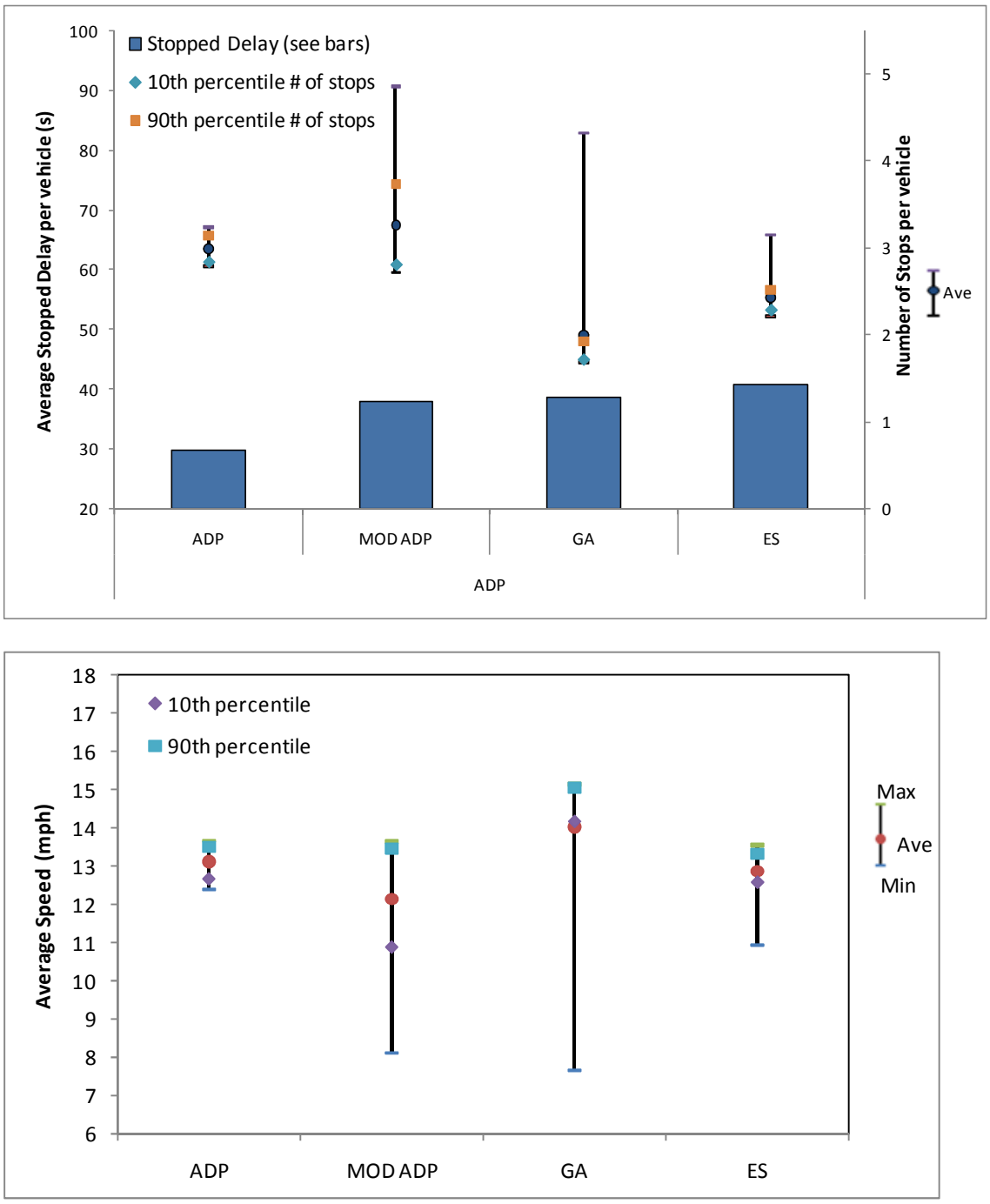

Figure 6.12. Average Vehicle Speeds, number of stops, and stopped delay for Case 2

The performance of the four methods in terms of the average number of stops and the average speeds is shown in Figure 6.12. The signal timings from GA and ES showed improved performance over ADP and modified ADP for both MOPs, mainly due to the effects of signal coordination. As presented in Chapter 5, GA and ES coordinated many of the movements in the modified Springfield network when the volumes at the entry links were 750 vehicles per hour per lane. Therefore, higher speeds and less number of stops were observed, with the exception of a three cases in which blockages prevented vehicles from crossing an intersection.

The animation from the simulation packages confirmed the coordination found by GA and ES. Similar cycle lengths, longer green times and adequate offsets between adjacent intersections also provided such indications. Some corridors were more benefited than others. For example the corridors with three lanes per direction (say, the two upper corridors in the E-W direction in the modified Springfield network) were an example of this situation. Thus, the GA algorithm favored directions that had entry links with greater number of lanes, as this would increase the throughput and reduce the overall number of vehicles queued.

Coordination was not explicitly a goal in the ADP formulation, as communication between intersections was not allowed, but given the variations in cycle lengths from one intersection to the other, coordination emerged at some points of the study period and also favored the performance of the signals to some (but lesser) degree.

Similar to the small network, the queue lengths were also monitored for this case, but since the entering volumes were lower than the capacity of the network, the results showed favorable performances for the average simulation run. More specifically, the percentage of time that the average links reached more than 80% of their capacity (both the links carrying entering volumes and those inside the network) was lower than 5% for all strategies.

On the other hand, the links were also monitored for queues equal to zero. This could be an indicator of proper distribution of green times between competing volumes and also of effective use of green. Results showed that on the average the left-turn pockets did not have queue for more than 70% of the time, and this measure was in the order of 20% for the

through links at the entering points and close to 40% for the other links. All strategies showed similar performance in this regard.

Overall, results show that the four methods had acceptable performance in this case, with volumes near saturation at some of the intersections at the edge of network. However, GA and ES had better average performances mostly due to the explicit management of coordination, which takes place by incorporating the offsets into the optimization process. This was observed in the lower number of stops, greater average speeds, and lower delays.

6.3 Case 3 - Modified Springfield network in oversaturated conditions

In the modified Springfield network, when the traffic at entry points was 1000 vehicles per hour per lane, GA and ES resulted in lower average delays per vehicle inside the network than ADP and modified ADP as presented in Figure 6.13.a. However, these two methods metered vehicles at the entry points and did not let them into the network. In fact, that was the reason of a lower average delay inside the network. Taking into account the effect of vehicles delayed before they entered the network, resulted in the delays in Figure 6.13.b. As shown in the figure, ADP and modified ADP resulted in lower total average delay and consequently greater number of vehicles in the network.

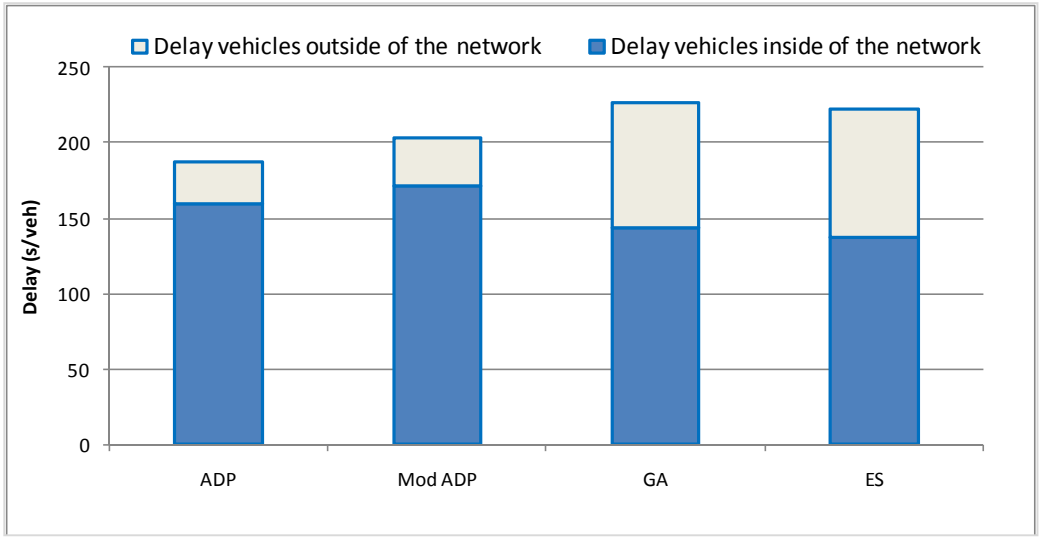

Average delay inside and outside of the network

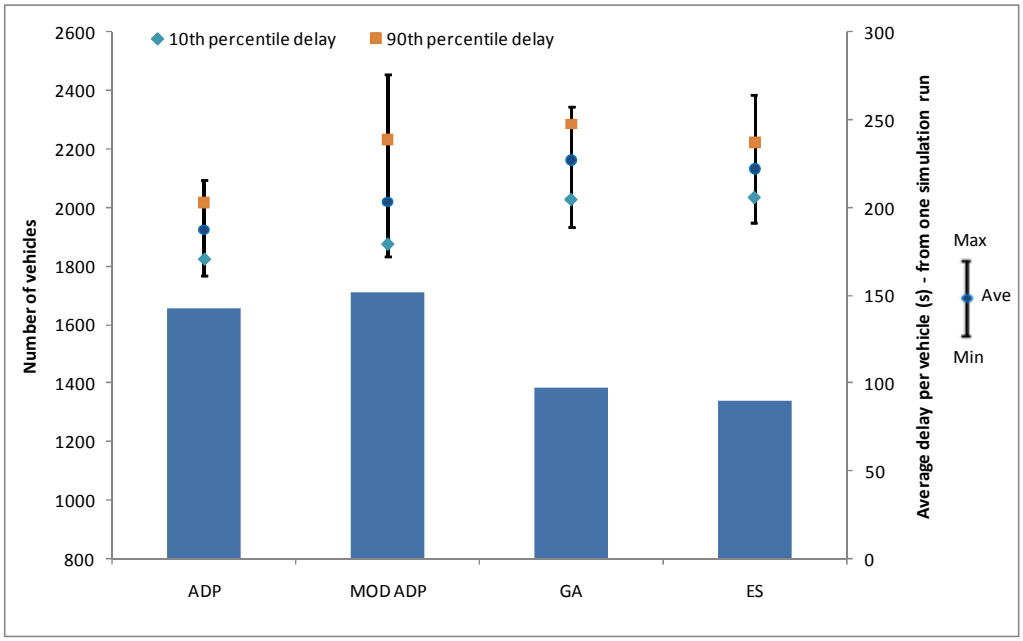

Average Delay and Network Congestion

Figure 6.13. Average Delay and Network Congestion for Case 3.

As presented in Table 6.3, for all methods the contribution of vehicles outside the network to delay was significant. However, for GA and ES this contribution was

significantly more than that for ADP and modified ADP, showing the effect of metering traffic at the entry points.

Table 6.3. Delay of Vehicles Outside the Network for Case 3

		ADP	MOD ADP	GA	ES
Vehicles delayed outside of the network (at entry points)	Min	1164.8	1231.72	1317.68	1366.4
	Average	1242.459	1307.1	1428.8	1427.3
	Max	1335.88	1384.32	1505.84	1531.04
Cummulative delay (s) of vehicles delayed outside of the network	Min	128231	131158.72	425265.1	451000.48
	Average	188500.1	213725.0	558197.6	572357.5
	Max	263515.8	422326.24	676083	675469.76
Average Ratio Delay vehicles outside/Total delay		**14.9%**	**15.6%**	**36.4%**	**38.2%**

Similar to delay, since GA and ES metered the vehicles at the entry points, the number of vehicles that were processed by them was lower than that of ADP. System throughput for modified ADP was similar to that for GA and ES and lower than ADP. In Figure 6.14 the network throughput for different algorithms is shown.

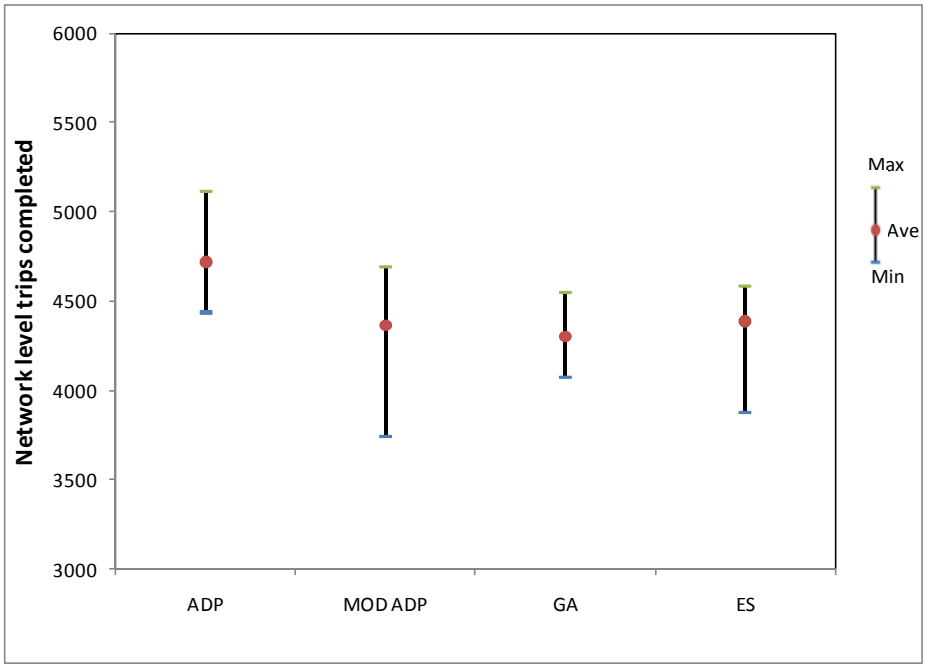

Figure 6.14. Network Throughput (Trips Completed) for Case 3

Since GA and ES did not let too many vehicles enter the network, they could maintain better level of service inside the network as the average speed for GA and ES methods was higher than those for ADP and modified ADP cases. In addition, the number of stops inside the network for GA and ES methods was lower than those for ADP and modified ADP algorithms. In fact, GA and ES could coordinate some of the signals in the oversaturated condition as discussed in Chapter 5. Average speeds, number of stops, and stopped delay are shown in Figure 6.15.

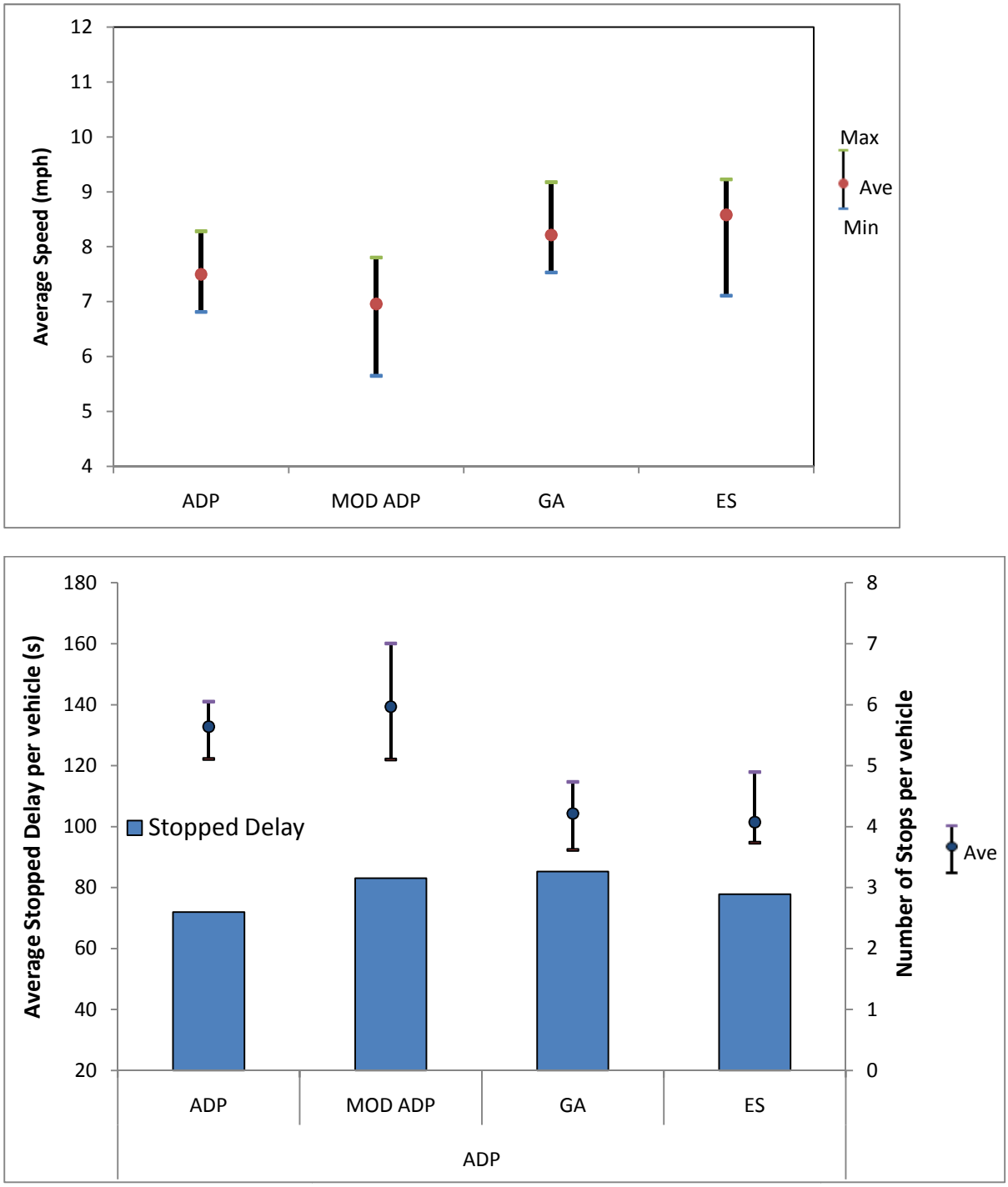

Figure 6.15. Average Vehicle Speeds, number of stops, and stopped delay for Case 3

Properly managing the queues is extremely important in oversaturated condition. The reason is that in this condition, if not managed properly, queues start growing and will eventually block the upstream intersections. If this blockage continues it can eventually cause

a gridlock which leads to significant increase in delays and loss in system throughput. Figure 6.16 shows maximum queue length at entry links of the network.

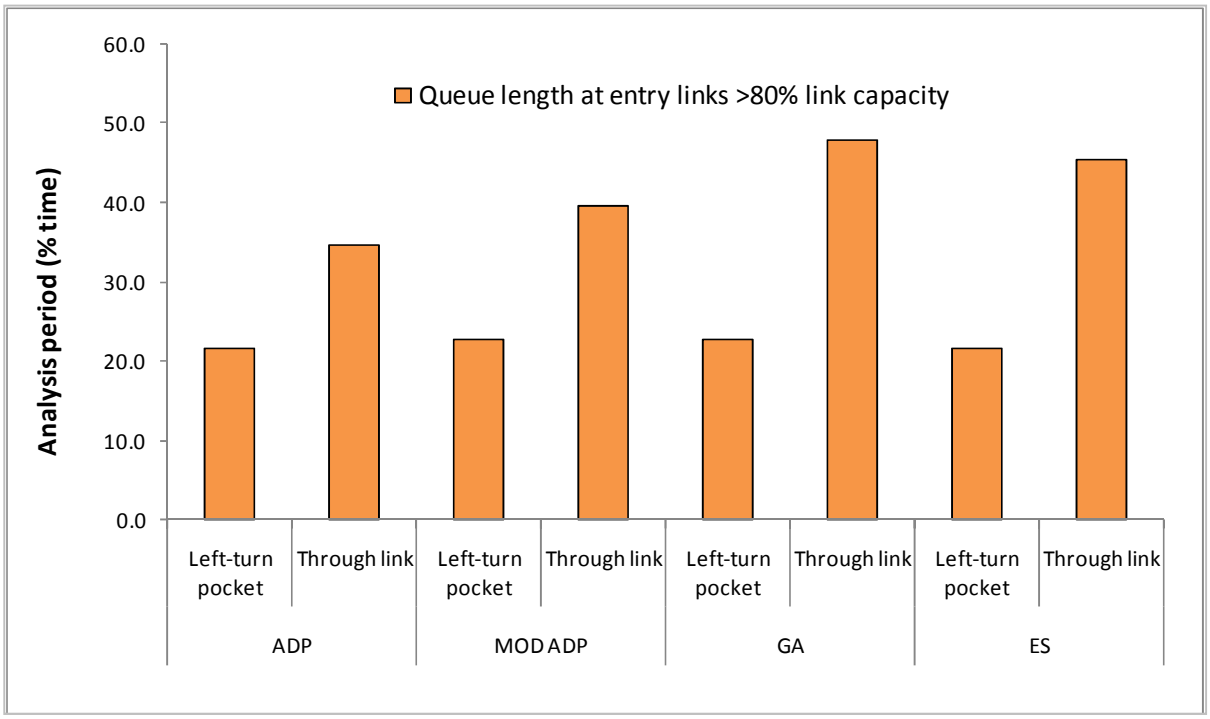

Figure 6.16. Potential Queue Overflows at Entry Links for Case 3

As expected, ADP and modified ADP resulted in fewer blockages at the entry links compared to GA and ES. This was due to the fact that GA and ES tended to meter the traffic at entry points resulting in longer queue in those links. On the other hand, GA and ES resulted in less instances of long queues inside the network compared to ADP and modified ADP. This is shown in Figure 6.17.

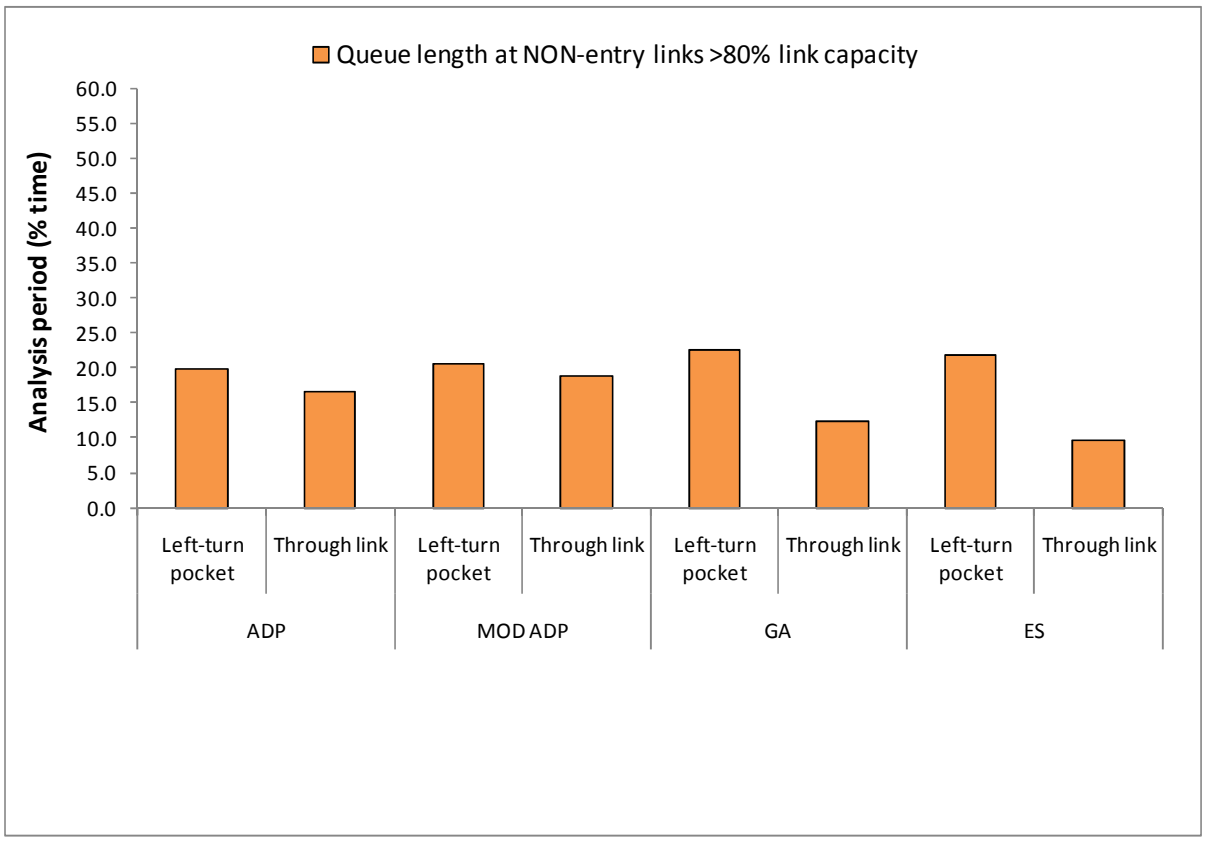

Figure 6.17. Potential Queue Overflows at NON-Entry Links for Case 3

In addition to the general measures of performance, the extreme values of the delay were also monitored. This analysis reveals the least-favored movements and the amount of delay for vehicles in such routes, as well as potential limitations on the applicability of certain strategies. Table 6.4 shows the average, maximum, and minimum number of vehicles with delays (per link) greater than 300 seconds, as well as the maximum delay in a single link, for all strategies.

Table 6.4. Maximum Delays per Link and Vehicles with Delays Greater than 300 Seconds for Case 3

Strategy	Statistic	Max Delay in one link (s)	# of Vehicles with delay >300s in one link
ADP	Min.	288	0
	Ave.	**421**	**26**
	Max.	616	117
MOD ADP	Min.	328	1
	Ave.	**480**	**60**
	Max.	764	390
GA	Min.	379	10
	Ave.	**530**	**57**
	Max.	754	142
ES	Min.	371	17
	Ave.	**498**	**41**
	Max.	728	93

6.4 Computational effort

The amount of time required to obtain the solutions presented in this section was also considered. Recall that the GA and ES methods are based on a search of the solution space and select one (solution) for the entire study period, whereas ADP learns over time based on the states that are visited and makes a decision every 2 seconds.

This gives ADP a clear advantage over the GA and ES because the algorithm has a solution soon after the learning process starts (it is an any-time algorithm), and the action-selection convergence was achieved in short time periods. In fact, the simulations were initiated with no previous learning and the ADP tables accumulated the value of each state as the 31 replications were executed in VISSIM. The approximated amount of time needed for the ADP to find the solutions shown in this study was in the order of 4 hours of CPU time using a PC with dual-core processors (2.4 GHz) and 4GB of memory. This was the time needed for VISSIM to complete the 31 simulation runs, thus ADP did not require any prior training to find the solutions.

GA and ES each make 60,000 simulation runs to find near optimal solution. Each simulation run in CORSIM needs around 5 seconds of CPU time. As a result, to find near optimal answer, GA and ES required around 300,000 seconds or around 3.5 days. GA and ES runs were performed on a PC with quad-core processors (2.67 GHz) and 3 GB of memory. It is noted that for the same network, each VISSIM simulation run takes 4 minutes and this was the main reason of not choosing VISSIM to interface with GA and ES.

6.5 Knowledge requirements

The knowledge and time needed to utilize the methodologies of this study, in terms of learning the techniques (ADP, GA, and ES), coding, and calibration are discussed in this section.

It is difficult to quantify the amount of time required to learn these techniques, considering that the background knowledge for ADP is very different from that used in GA or ES. However, it is possible to say that prior experience with Markov decision processes and machine learning will help fully understanding ADP, whereas knowledge in search and optimization heuristics may help understanding GA and ES. Also, once the user understands GA, it is fairly straightforward to implement an ES algorithm, and vice versa.

In terms of available literature and past experiences using each of these techniques, genetic algorithms are a good base point to start the implementation of ADP, whereas numerous past experiences with GA might be very useful for the development of the algorithm for a particular network.

In terms of inputs, ADP requires a frequent estimation of the state of the system – which in this case was the queue length of each approach and the phase duration. For the computer modeling, this requirement could be satisfied by the addition of vehicle detectors at multiple points in each link, or alternatively by reading the queue status from the simulation in real time (through an API). Of these two methods, the former was adopted in this study. On the other hand, the GA and ES techniques evaluate the signal timings at the end of each simulation, and thus they do not require inputs from detectors.

Calibration may be needed for the three methods. For ADP, decreasing learning rates (α) are needed as well as a discount factor (γ) and a factor (λ) if eligibility traces are used. Lastly, the user needs to define a cost function that describes what actions are desired (such as the one used in this study). In general, standard values used in the literature are good starting points, but a sensitivity analysis may reveal improvements depending on the specific problem. Calibration of GA and ES is fairly easy. The reason is that both algorithms have an area in which the parameters yield an adequate search in the solution space (or "sweet spot"), and the ranges of these values are easy to find.

6.6 Potential for field implementation

There is true potential for these techniques in real-world applications. For ADP, the advantages of being suitable for real-time decision-making make it appropriate for traffic fluctuations and adaptive control. Also, with the advance of detection technologies and in-vehicle equipment, knowing the state of the system at all times is possible. In fact, there are adaptive systems currently in operation that monitor the back of queue via video detection and determine the state of the system to make decisions. Additional algorithm development and testing under variable demands and in different network configurations are required for further analysis.

As mentioned before, run time for GA and ES is significantly longer for real-time application. As a result, if GA or ES are coupled with a microscopic traffic simulation, they will not be able to determine the signal timing parameters in a reasonable time. Other strategies such as the use of mesoscopic simulators or even models at the macroscopic level could be explored to reduce the running time for field implementations.

CHAPTER 7. QUEUE MANAGEMENT ANALYSIS

Queue management was evaluated based on a series of MOPs that accounted for the efficient utilization of green time and the probability of queue overflows at the upstream intersection. This later MOP is similar to the analysis presented before on queues greater than 80%, but it shows the amount of time that queues actually exceeded the link capacity by having a length greater than the link itself.

On the other hand, the efficient utilization of green times was measured in terms of average vehicle headway during the green phase (in seconds) and analyzed based on the fact that processing vehicles at saturation headway (set at 1.9 seconds) is expected to result in an efficient operation. Moreover, processing vehicles at saturation headway does not only indicate that there is no "unused green", but also shows that the downstream links have capacity to receive the departing vehicles. When the downstream link does not have capacity to receive the vehicles coming from the upstream link, the departure headways would be less than the saturation headway; thus the departure rate is less than the saturation flow.

A third MOP that was explored in queue management is related to the actual congestion level of the network on the entry and non-entry links, and also on the through and left-turn movements. This factor was called "queue occupancy" and was calculated as the ratio of the summation of all queues to the total length of the links, or $\frac{\sum_i q_i}{\sum_i L_i}$ (where $q_i$is the queue length at link *i*, and L_i is the length of link *i)*. Lastly, a fourth MOP shows the global congestion using network-level queue occupancy, which takes into account all links in the network together. This measure shows the degree of storage capacity utilization with respect to vehicles that are experiencing significant delay (in queue).

7.1 Case 1 - Network of 9 intersections in oversaturated conditions

For the small network of 9 intersections, the green utilization efficiency in terms of average headway during the green phase is shown in Table 7.1. The highlighted cells show the most favorable methods within each of the three optimization methods, which are also those with the lowest vehicle headway.

Table 7.1. Green Utilization Efficiency for Case 1

Method		Average Vehicle Headway during Green Phase (s)					
		All Network		Entry Links		Non-entry Links	
		Through	Left	Through	Left	Through	Left
ADP	ADP	1.91	2.00	1.85	1.88	1.93	2.05
	ADP ELIG	1.95	2.04	1.89	1.92	1.98	2.09
	ADP MOD1	1.98	1.96	1.91	1.90	2.01	1.98
	ADP MOD2	1.93	2.18	1.87	2.10	1.96	2.21
	ADP MOD3	1.93	2.00	1.86	1.96	1.96	2.01
ES	ES	1.97	1.80	1.89	1.73	2.01	1.82
	ES10	2.19	1.75	2.03	1.75	2.26	1.75
	ES20	2.21	1.76	2.02	1.75	2.28	1.77
GA	GA	1.95	1.80	1.88	1.73	1.98	1.83
	GA10	2.18	1.75	2.02	1.73	2.23	1.75
	GA20	2.16	1.75	2.01	1.73	2.21	1.76

In general, entry links had shorter vehicle headways than non-entry links, showing that the demand on these approaches was higher and the allocated green time processed a greater number of vehicles per unit of time. Comparing through movements to left turns, the ADP shows shorter headways for through vehicles than for left, and the opposite was true for ES and GA. It is noted that some of the average vehicle headways are shorter than the saturation headway (sat to 1.9 seconds) and this was the result of vehicles using more time of the yellow transition (to complete the movement) compared to the lost time at the beginning of the green phase. Thus, in practice for some movements the effective green was somewhat longer than the actual time allocated to the green phase.

Overall, the three highlighted methods (ADP, GA, and ES) obtained vehicle headways at the network level that were very close to the saturation headway, indicating an effective utilization of the green time.

A second MOP for the queue management analysis was the amount of time (in seconds) that the queues exceeded the length of the links and created blockages in the upstream intersections (or the entry points at the network edge). A summary of this MOP is shown in Table 7.2.

Table 7.2. Time Queue Exceeded Length of the Links for Case 1

Method	Average Time that Queue Exceeded Length of Links (s)			
	Entry Links		Non-entry Links	
	Through	Left-turn	Through	Left-turn
ADP	0	0	0	0
ADP ELIG	0	0	0	0
MOD 1	0	0	0	0
MOD 2	0	0	0	0
MOD 3	0	0	0	0
ES	0	2	0	0
ES10	0	66	0	0
ES20	0	65	0	0
GA	0	3	0	0
GA10	0	78	0	0
GA20	0	68	0	0

It is observed that the only points in the network in which the queue was longer than the links was at the entry links and more specifically at the left-turn lanes. However, this situation was detected in only a small portion of the 900-second runs and in all cases it represented less than 10% of the analysis period.

The queue occupancy at the link level is shown in Table 7.3. Recall that these values were found by dividing the queue length by the length of the link where the queue starts.

Table 7.3. Queue Occupancy for Case 1

Method		Queue Occupancy			
		Entry Links		Non-entry Links	
		Through	Left	Through	Left
ADP	ADP	0.47	0.18	0.12	0.14
	ADP ELIG	0.49	0.18	0.12	0.14
	ADP MOD1	0.55	0.15	0.13	0.08
	ADP MOD2	0.49	0.15	0.12	0.07
	ADP MOD3	0.48	0.18	0.11	0.10
ES	ES	0.50	0.27	0.10	0.12
	ES10	0.50	0.53	0.08	0.25
	ES20	0.50	0.53	0.10	0.26
GA	GA	0.48	0.29	0.11	0.12
	GA10	0.47	0.54	0.09	0.25
	GA20	0.47	0.53	0.10	0.25

The methods that had the "best" green utilization efficiency within each group are highlighted. The queue occupation for entry and non-entry links was very different, as expected, with queues in the entry links that are at least double of those in the inner links. Note that on average the different methods did not load the links by more than 15% of their capacity for the through or left movements in the non-entry links. Here it is evident that the main difference between the overloading (ES10, ES20, GA10, and GA20) and the non-overloading strategies for ES and GA was the length of the queues in the left turn lanes, which ultimately resulted in the former group having lower performance for the entire network.

A summary of the network-level queue occupancy is shown in Table 7.4. There is a clear tendency for the algorithms not to allow the network to have queues longer than 20% of its storage capacity. For the strategies designed to overload the network, the global utilization factor increased on average 0.25-0.26.

Table 7.4. Network-level Queue Occupancy for Case 1

Method	Network-level Queue Occupancy		
	Average	Max	Min
ADP	0.20	0.22	0.18
ADP ELIG	0.21	0.23	0.19
MOD 1	0.20	0.22	0.19
MOD 2	0.19	0.20	0.17
MOD 3	0.19	0.20	0.18
ES	0.20	0.22	0.19
ES10	0.25	0.27	0.23
ES20	0.26	0.28	0.24
GA	0.21	0.22	0.19
GA10	0.25	0.27	0.22
GA20	0.25	0.27	0.23

7.2 Case 2 - Modified Springfield network in close-to-saturation conditions

A similar set of MOPs to those described for the small network were also investigated for Cases 2 and 3 (modified Springfield network). First, the efficiency of green utilization for Case 2 is described in terms of the average vehicle headway during the green phase (Table 7.5).

Table 7.5. Green Utilization Efficiency for Case 2

Method	Average Vehicle Headway during Green Phase (s)					
	All Network		Entry Links		Non-entry Links	
	Through	Left	Through	Left	Through	Left
ADP	2.12	21.26	2.10	21.84	2.13	21.16
MOD ADP	2.21	21.91	2.15	22.18	2.23	21.86
GA	2.27	20.27	2.21	16.92	2.28	20.88
ES	2.26	22.16	2.18	23.31	2.29	21.95

Vehicle headways for the four methods were above the saturation headway, but this was expected since the entering volumes were lower than the saturation level. In particular, headways for left turns are very high as the demand is much lower (10% of the total demand) in comparison to the through traffic and the movement is permitted, thus they share the same green times. Also, the undersaturated operation allowed more left turns to be processed using gaps in the opposing traffic. The presence of very short left-turn queues is later confirmed in this section by looking at the occupancy of the left turn pockets, which was very low.

In this particular case, queue management is not expected to be as critical in terms of green efficiency, as with the back of the queues, which are analyzed next, in Table 7.6.

Table 7.6. Time Queue Exceeded Length of the Links for Case 2

Method	Average Time that Queue Exceeded Length of Links (s)			
	Entry Links		Non-entry Links	
	Through	Left-turn	Through	Left-turn
ADP	0.2	0.3	4.5	0.9
MOD ADP	4.4	1.0	61.4	1.5
GA	7.2	6.8	32.6	8.0
ES	4.5	5.5	30.7	9.9

From Table 7.6 it is noted that at some points of the analysis period both the through movements and the left-turns could have created blockages. These temporary blockages were more prolonged at non-entry links, and more specifically at intersections 5 and 6, where three-lane one-way streets intersected. Additional analysis at the link level showed that another critical location was the westbound traffic at intersection 1 and the southbound traffic at intersection 2 (both of them three-lane, one-way streets).

Queue occupancy was also obtained for Case 2, as shown in Table 7.7. The queue length with respect to the length of the links was significantly lower than in Case 1 (given the undersaturated conditions) even though the links were significantly shorter. Results from Table 7.7 are in accordance with Table 7.6, showing that low average queue resulted in low probability of blockages.

Table 7.7. Queue Occupancy for Case 2

Method	Queue Occupancy			
	Entry Links		Non-entry Links	
	Through	Left	Through	Left
ADP	0.18	0.04	0.20	0.04
MOD ADP	0.23	0.05	0.21	0.04
GA	0.25	0.06	0.14	0.07
ES	0.23	0.05	0.21	0.04

Thenetwork-level queue occupancy for the four methods is shown in Table 7.8. Results indicate that on average from 14% to 17% of the network length was composed of queued vehicles, with maximum values form a single run below 30%.

Table 7.8. Network-level Queue Occupancy for Case 2

Method	Network-level Queue Occupancy		
	Average	Max	Min
ADP	0.15	0.17	0.14
MOD ADP	0.17	0.27	0.14
GA	0.14	0.26	0.11
ES	0.17	0.21	0.15

7.3 Case 3 - Modified Springfield network in oversaturated conditions

This case was expected to provide distinctive details on the operating strategies using the four different methods. The oversaturated conditions and short spacing between intersections, in addition to a variety of lane configurations, provide a very challenging scenario for the algorithms.

The first queue management MOP is the efficient utilization of green time, expressed as the average vehicle headway, as shown in Table 7.9. It shows that some efficiency was lost in this case compared to the undersaturated case. This may seem counterintuitive at first because higher demand should produce less unused green, but it was mainly the result of the following four situations: 1) blockages due to queue overflow in the crossing street, which prevented vehicles from reaching the downstream intersection; 2) extending green to process long queues and prevent blockages, at the cost of platoon dispersion and lower efficiency; 3) disparity of volume demands on two-way roadways, generating unused green in the direction with lower traffic; and 4) the priority given to streets with greater number of lanes, as they could process more vehicles, but also at the cost of platoon dispersion and greater headways.

Table 7.9. Green Utilization Efficiency for Case 3

Method	Average Vehicle Headway during Green Phase (s)					
	All Network		Entry Links		Non-entry Links	
	Through	Left	Through	Left	Through	Left
ADP	2.33	10.44	2.24	10.04	2.35	10.51
MOD ADP	2.51	10.91	2.39	10.28	2.55	11.02
GA	2.72	12.92	2.28	11.32	2.85	13.21
ES	2.59	12.56	2.19	10.93	2.71	12.85

The amount of time that the links had queues longer than the storage capacity is shown in Table 7.10. As expected, on average both the entry and non-entry links experienced some blockages, which most of the time did not result in gridlocks. Note that longer blockages were found at the entry links with GA and ES, but the opposite was true for the non-entry links where blockages were longer in ADP and modified ADP. This is also evidence of a key difference in the results from these methods, as GA and ES did perform a more intensive metering at some intersections, and ADP allowed more vehicles inside of the network.

Table 7.10. Time Queue Exceeded Length of the Links for Case 3

Method	Average Time that Queue Exceeded Length of Links (s)			
	Entry Links		Non-entry Links	
	Through	Left-turn	Through	Left-turn
ADP	73.8	572.5	233.5	465.0
MOD ADP	89.5	603.8	305.4	483.3
GA	113.8	615.8	215.0	542.1
ES	107.8	580.5	150.8	523.2

The queue occupancy of the links was grouped by entry and non-entry links, as well as by the type of movement, as it is shown in Table 7.11. A similar picture to that described in the previous MOPs is also found from Table 7.11. The through entry links with ADP and MOD ADP were slightly less congested than those in GA and ES, with average queues as long as 70% of the link capacity. On the other hand, non-entry through links with ADP and MOD ADP reached about 40% capacity inside the network, compared to close to 30% with GA and ES.

Table 7.11. Queue Occupancy for Case 3

Method	Queue Occupancy			
	Entry Links		Non-entry Links	
	Through	Left	Through	Left
ADP	0.67	0.71	0.41	0.66
MOD ADP	0.70	0.74	0.40	0.66
GA	0.73	0.80	0.31	0.72
ES	0.72	0.73	0.27	0.68

Left-turning links were highly congested with queues close to 70% of the link storage capacity even inside the network. In fact, a more detail analysis of the queues at the link level

showed that the majority of the top 10% most congested links for all four strategies were left-turns, and in particular those in intersections 15, 16, 19, and 20. Recall that at this location all four approaches had left-turning lanes and that all of them operated on a "permitted" basis.

Lastly, the network-level queue occupancy is shown in Table 7.12. Even though the network is oversaturated, the length of queues in all the links together was on average lower than 50% of the storage capacity of the network. These results are very different from those in undersaturated conditions, where the global storage utilization factor was lower than 20%, and may be a first indication of an upper bound for this factor in this particular network.

Table 7.12. Network-level Queue Occupancy for Case 3

Method	Network-level Queue Occupancy		
	Average	Max	Min
ADP	0.46	0.51	0.40
MOD ADP	0.47	0.53	0.42
GA	0.40	0.47	0.35
ES	0.38	0.44	0.33

For queue management purposes, all four measures mentioned in this Chapter provide important information for understanding the operation of a set of signal timings. Green utilization efficiency and queue occupancy should be used simultaneously, not as separate factors. If the green time is not efficiently used it is highly likely for the queues in the links to start growing and eventually blocking an upstream intersection, and if this happens in combination with high level of link occupancies the network is likely to reduce the number of vehicles that can be processed.

One expects that number of trips in Case 3 to be higher than that in Case 2 since traffic demand in Case 3 was higher; However, results revealed that the number of trips completed in Case 2 was higher than that for Case 3, and this can be observed in the green utilization efficiency and queue occupancy. By increasing traffic demand from 750 vehicle per hour per lane to 1000 vehicle per hour per lane, queues started to grow in the network and occasionally blocked upstream intersections. This resulted in a less efficient use of green time as reflected by a greater green utilization factor (headways greater than the saturation headway – set at 1.9 seconds). In addition, greater demand increased the queue occupancy of

the network. This suggests that allowing more vehicles in the network may not be the best action for all traffic conditions. In fact, all vehicles could enter the network up to a certain traffic demand; however, if more vehicles are allowed in the network beyond that point, the network may not be able to process them. This may result in a decrease in number of trips completed, and in an increase in average travel delay both inside the network and at the borders.

CHAPTER 8. CONCLUSIONS

Three methods were used to find the optimal signal timings for two transportation networks: Genetic Algorithms (GA), Evolution Strategies (ES), and Approximate Dynamic Programming (ADP). While GA and ES are meta-heuristics for searching the solution space, ADP tries to learn the best actions after knowing the state of the system. ADP has potential for real-time implementation, whereas GA and ES are more suitable for development and evaluation of various strategies that can be selected in real-time traffic control.

The formulations from the three methods were described, including variations that explored different approximations to the problem solution. Two case study networks were used. The first one was a small hypothetical network of 9 oversaturated intersections. On this network, GA, ES methods were use to find optimal solutions for three network loading conditions (no overloading, 10%, and 20% overloading). Also two variations of ADP (no eligibility traces and eligibility traces) and three modified ADP algorithms were tested for the small network. Results indicated that GA and ES with no overloading and two variations of ADP and their modifications found signal timings that resulted in similar network performances. For these four cases, the average delay was between 215 and 226 seconds per vehicle. The ADP Modification 3 resulted in the lowest average delay and ADP with eligibility traces resulted in the highest. System throughput was also similar and ranged from 2095 vehicles (ES with 20% overloading) to 2320 vehicles (ADP with no eligibility traces). When the network was overloaded by 10% or 20%, the average delay per vehicle was significantly increased while system throughput was at the same level or slightly lower.

In comparison, the signal timings (for the small network) found by the best strategies were in some cases significantly different from each other. The strategies proposed by GA and ES were similar and resulted in cycle lengths that fluctuated between 78 and 98 seconds, with identical averages of 85 seconds. On the other hand, the ADP strategies (with and without eligibility traces), suggested cycle lengths of 85 to 107 seconds when left turns phases were displayed and cycle lengths of 50 to 63 seconds without left turn phases.

For the modified Springfield network, when the volume at the entry links was 750 vehicles per hour per lane GA (70.3 s) and ADP (75.8 s) found signal timings that resulted in shorter average delay than ES (78.7 s) and modified ADP (85.62 s). Network throughput for GA (4987 vehicles), ES (5005 vehicles), and ADP (4981 vehicles) was similar and slightly higher than that for modified ADP (4746 vehicles). Higher throughput and lower delay for GA and ES was expected since they were optimizing the offsets in addition to signal timing parameters and as a result coordinated several intersections of the network. ADP on the other hand was responding to the current network assuming the intersections were not interconnected. The signal coordination resulted in less number of stops in the network and increased average speed. Thus, average number of stops for GA (2.0 stops) and ES (2.4 stops) were fewer than that for ADP (3.0) and its modification (3.3). In addition, GA (14.0 mph), ES (12.9 mph), and ADP (13.1) resulted in a higher average speed in the network than modified ADP (12.1 mph).

When the entry volumes were set to 1000 in the modified Springfield network, GA and ES could coordinate some of the signals of the network. As a result, average delay inside the network for GA (144 s) and ES (137 s) was shorter than that for ADP (159 s) and modified ADP (171 s). However, GA and ES metered vehicles at the entry links more than ADP and its modification and did not let too many vehicles enter the network. This resulted in a larger average delay inside and outside of the network for GA (227 s) and ES (222 s) compared to ADP (187 s) and modified ADP (203 s). Since GA and ES let fewer number of vehicles in the network they could process less vehicles and network throughput for ADP (4718 vehicles) was more than that for GA (4302 vehicles) and ES (4388 vehicles). On the other hand, since inside the network was not that congested, the average number of stops was lower for GA (4.2 stops) and ES (4.1 stops) compared to ADP (5.1 stops) and modified ADP

(5.1 stops), and average speed was higher (8.2 mph and 8.6 mph for GA and ES, 7.5 mph and 7.0 for ADP and modified ADP, respectively)

For queue management purposes, all four measures mentioned in Chapter 7 provide important information for understanding the operation of a set of signal timings. However, it is recommended to use the green utilization efficiency and queue occupancy simultaneously, not as separate factors. If the green time is not efficiently used it is highly likely for the queues in the oversaturated links to start growing and eventually blocking an upstream intersection, and if this happens in combination with high level of link occupancies the network is likely to reduce the number of vehicles that can be processed.

The queue management analysis showed that to get the best network performance in the oversaturated condition, the green utilization efficiency for protected movements (through or left-turns) should be close to saturation headway (1.9 seconds in this study).

In addition, it was found that letting all the vehicles enter the network may not be the best action for all traffic conditions. Vehicles could enter the network up to a certain traffic demand, but beyond this point, the network may not be able to process them and it could result in blockages or gridlocks. This may in turn result in a decrease in the number of trips, and an increase in average travel delay both inside the network and at the borders. Therefore, whenever traffic demand is beyond this optimal level, the additional traffic demand should be metered to prevent a decrease in the network throughput.

Future work to improve the methods described in the report, particularly for real-world applications, is needed. Several topics can be further studied for advancing the state-of-the-practice in traffic signal control, including: 1) reduction in the required running time for GA and ES, 2) improvements in the algorithm for ADP regarding the state representation and the learning functions, 3) the long term performance of the algorithms, and 4) extended capabilities such as communication between intersection and augmented set of constraints to account for known issues in real-world scenarios.

Reference

Beyer, H.-G. (2001). The Theory of Evolution Strategies. Heidelberg: Springer.

Cai, C., Kwong Wong, C., and Heydecker, B.G. (2009) Adaptive Traffic Signal Control Using Approximate Dynamic Programming, Transportation Research Part C: Emerging Technologies, vol. 17, pp. 456-474.

Chang, T.-H., & Sun, G.-Y. (2004). Modeling and Optimization of an Oversaturated Signalized Network. Transportation Research Part B , 38, 687-707.

Daganzo, C. (1992). The Cell Transmission Model. Part I: A Simple Dynamic Representation Of Highway Traffic. Berkeley, CA: Research Reports, California Partners for Advanced Transit and Highways (PATH), Institute of Transportation Studies, UC Berkeley.

D'Ans, G. C., & Gazis, D. C. (1976). Optimal Control of Oversaturated Store-and-Forward Transportation Networks. Transportation Science , 10 (1), 1-19.

Gartner, N.H. (1983) OPAC: a demand-responsive strategy for traffic signal control. Transportation Research Record 906, 75–81.

Gazis, D. C. (1964). Optimum Control of a System of Oversaturated Intersections. Operation Research , 12 (No. 6), 815-831.

Gazis, D. C., & Potts, R. B. (1965). The Oversaturated Intersection. Second International Symposium on the Theory of Road Traffic Flow (pp. 221-237). Paris: Organization for Economic Cooperation and Development.

Girianna, M., & Benekohal, R. f. (2002). Dynamic Signal Coordination for Networks with Oversaturated Intersections. Transportation Research REcord (1811), 122-130.

Goldberg, D. E. (1989). Genetic Algorithms in Search, Optimization, and Machine Learning. Boston, MA, USA: Addison-Wesley Longman Publishing Co., Inc.

Li, Z., & Chang, G.-l. (2010). Modeling Arterial Signal Optimization with Enhanced Cell Transmission Formulation. Transportation Research Board. Washington DC: Transportation Research Board.

Lieberman, E., Chang, j., Bertoli, B., & Wuping, X. (2010). New Signal Control Optimization Policy for Oversaturated Arterial Systems. Transportation Research Board. Washington DC: Transportation Research Board.

Lo, H. L., & Chow, H. F. (2004). Control Strategies for Oversaturated Traffic. Journal of Transportation Engineering ASCE , 130 (4), 466-478.

Longley, D. (1968). A Control Strategy for a Congested Computer Controlled Traffic Network. Transportation Research , 2, 391-408.

Michalopoulos, P. G., & Stephanopoulos, G. (1977). Oversaturated Signal System with Queue Length Constraints-I. Transportation Research , 11, 413-421.

Park, B., Messer, C. J., & Urbanik II, T. (2000). Enhanced Genetic Algorithm for Signal-Timing Optimization of Oversaturated Intersections. Transportation Research Record (1727), 32-41.

Peng, J., Williams R. J. (1996) Incremental Multistep Q-learning. Machine Learning, 22, 283-290.

Putha, R., Quadrifoglio, L., & Zechman, E. (2010). Using Ant Colony Optimization for Solving Traffic Signal Coordination in Oversaturated Networks. Transportation Research Board. Washington DC: Transportation Research Board.

Robertson, D.I., Bertherton, R.D. (1974) Optimum control of an intersection for any known sequence of vehicular arrivals. In: Proceedings of the second IFACIFIP-IFORS Symposium on Traffic Control and Transportation system, Monte Carlo.

Schrank, D., & Lomax, T. (2009). Urban Mobility Report. University Center for Mobility. Texas Transportation Institute.

Schwefel, H.-P. (1965). Kybernetische Evolution als Strategie der exprimentellen Forschung in der Strömungstechnik. Berlin: Technical University of Berlin.

Singh, S. P. and Sutton, R. S. (1996). Reinforcement learning with replacing eligibility traces. Machine Learning, 22:123-158

Singh, M. G., & Tamura, H. (1974). Modelling and Hierarchical Optimization for Oversaturated Urban Road Networks. International Journal for Control , 20 (6), 913-934.

Teodorvic D., V. Varadarajan, J. Popovic, M. R. Chinnaswamy, S. Ramaraj,. Dynamic Dynamin programming—neural network real-time traffic adaptive signal control algorithm. Annals of Operation Research, pp-123-131, 2006.

Watkins, C. J. C. H. and Dayan, P. (1992) Q-learning. Machine Learning 8: 279-292

Xie, Y., Zhang, Y., & Li, L. (2010). Neuro-Fuzzy Reinforcement Learning for Adaptive Intersection Traffic Signal Control. Transportation Research Board. Washington DC: Transportation Research Board.

Xin, W., Chang, J., Bertoli, B., & Talas, M. (2010). Integrated Adaptive Traffic Signal Control with Real-time Decision Support. Transportation Research Board. Washington DC: Transportation Research Board.

Yuan, C., Yang, X., & Shen, F. (2006). Fixed Cycle Strategy in Oversaturated Network Traffic Control. the 6th World Congress on Intelligent Control and Automation, (pp. 8674-8678).

Zhang, L., Yin, Y., & Lou, Y. (2010). Robust Signal Timing for Arterials under Day-to-Day Demand Variations. Transportation Research Board. Washington DC: Transportation Research Board.